

Global Warming and the "impossible" Radiation Imbalance

Ad Huijser



SCC Publishing Michelets vei 8 B 1366 Lysaker Norway Abstract

Correspondence: ah@on.nl Vol. 5.3 (2025)

pp. 81-106

ISSN: 2703-9072

Any perturbation in the radiative balance at the top of the atmosphere (TOA) that induces a net energy flux into- or out of Earth's thermal system will result in a surface temperature response until a new equilibrium is reached. According to the Anthropogenic Global Warming (AGW) hypothesis which attributes global warming solely to rising concentrations of Greenhouse gases (GHGs), the observed increase in Earth's radiative imbalance is entirely driven by anthropogenic GHG-emissions.

However, a comparison of the observed TOA radiation imbalance with the assumed GHG forcing trend reveals that the latter is insufficient to account for the former. This discrepancy persists even when using the relatively high radiative forcing values for CO2 adopted by the Intergovernmental Panel on Climate Change (IPCC), thereby challenging the validity of attributing recent global warming exclusively to human-caused GHG emissions.

In this paper, Earth's climate system is analyzed as a subsystem of the broader Earth Thermal System, allowing for the application of a "virtual balance" approach to distinguish between anthropogenic and other, natural contributions to global warming. Satellite-based TOA radiation data from the CERES program (since 2000), in conjunction with Ocean Heat Content (OHC) data from the ARGO float program (since 2004), indicate that natural forcings must also play a significant role. Specifically, the observed warming aligns with the net increase in incoming shortwave solar radiation (SW_{IN}), likely due to changes in cloud cover and surface albedo. Arguments suggesting that the SW_{IN} trend is merely a feedback response to GHG-induced warming are shown to be quantitatively insufficient.

This analysis concludes that approximately two-thirds of the observed global warming must be attributed to natural factors that increase incoming solar radiation, with only one-third attributable to rising GHG-concentrations. Taken together, these findings imply a much lower climate sensitivity than suggested by IPCC-endorsed Global Circulation Models (GCMs).

Keywords: Global Warming; Radiation Imbalance; GHG-forcing; Climate Sensitivity; Ocean Heat Content.

Submitted 2025-07-19, Accepted 2025-08-22. https://doi.org/10.53234/scc202510/05

1. Introduction

In spring 2024, the Royal Dutch Metrological Institute (KNMI) published a new webpage centered around a picture of the growth in the radiation imbalance full of suggestive lines to make a claimed "acceleration" in global warming visible. Determining accelerations over periods of a few years in a climate with a relaxation time to changes of 3 to 5 years however, tends to speculation. The picture used, is taken from a paper with the title "Global warming in the pipeline" by Hansen et al [2]. These authors use even much longer relaxation times, based on the analyses of Global Circulation Models (GCMs). They claim that our climate is governed by processes strongly delaying the warming effects of forcings coupled to the growing concentration of Greenhous gasses (GHGs) like CO2. Their paper warns for future warming, even if we stop with the anthropogenic emissions now. At the same time, it is used as a justification for the very high climate sensitivities and accordingly, long relaxation times that these GCMs deliver. To help explain the significant difference between their GCM's output with much higher temperature trends

Science of Climate Change

than that are being (yet?) observed, they distinguish different climate sensitivities, a fast and a slow one. A rather complex concept for what is, at its core, a relatively simple thermal system.

This "relative simplicity" doesn't apply to localized weather phenomena, which even exhibit chaotic behavior. However, on a global scale and over longer periods of time, the average surface temperature of our climate system reacts similarly to that of a thermal system such as a pot of water on a stove: when the incoming heat is steady and below boiling, the system stabilizes when the heat loss (via radiation and convection) equals the input. Analogously, Earth's surface-atmosphere interface is the main absorber and emitter of heat. Reducing the "flame" (solar input) leads to cooling, regardless of the total heat already stored in the system. The system's average temperature will drop as well, as soon as the heating stops. So, no sign of any "warming in the pipeline" for such a simple system.

Yet Earth's climate system is inherently more complex due to its scale and the dynamics introduced by Earth's rotation and orbit. Solar heating occurs only half the time at any given location, and the Earth's surface is in constant rotation, with the solar heating peak moving at speeds of up to 0.5 km/s. Heat is therefore continuously redistributed across the globe via lateral atmospheric and oceanic flows. Averaged over time, these transports move heat from the Tropics (where most solar radiation is absorbed) to the Poles (which receive far less solar energy), with approximately 80% of the 5 PW carried by wind and the remainder by ocean currents [3]. These fluxes are partially equalizing the huge differences in the amount of incoming Solar radiation. Around the Equator, the radiation imbalance is highly positive, with about 40 W/m² more Sunlight coming in than Long-Wavelength radiation going out. Around the Poles we see the opposite, with a substantial negative balance in the order of about 100 W/m² by a higher flux out, than in. In average there is a (near) radiation balance that can be easily influenced by variations in both lateral heat flows. Consequently, changes in the amount of heat carried and/or changes in the path along which that heat is being transported, can easily influence the average surface temperature. Often, such changes are conveniently interpreted by AGW-proponents as being the result, rather than the cause of global warming. Those anthropogenic GHG-driven effects are by some even coupled to induce irreversible changes in our climate at so-called tipping points.

The two transport mechanisms, air and ocean, operate on different timescales. Air has a low specific heat capacity, but high wind speeds make it a fast medium for heat transfer. Oceans, by contrast, have a high specific heat capacity but move more slowly. The Atlantic Meridional Overturning Circulation (AMOC) with the well-known Gulf Stream carrying warm water from south to north, can reach speeds up to about 3 m/s. But its warm current remains largely confined to surface layers due to limited solar radiation penetration and gravity-induced stratification. With a path-lengths of up to 8,000 km and an average speed of 1.5 m/s, ocean heat takes approximately 2 months to travel from the Gulf of Mexico to the Arctic. This is comparable to the 1 to 2 months delay between solar input and temperature response in the annual cycle, suggesting that oceanic heat transport is part of the climate system's normal operation. Climate adaptation times from anthropogenic influences are estimated at 3 to 5 years. If "warming in the pipeline" exists, it must be buried in the much colder, deeper ocean layers.

ARGO float data since 2004 show substantial annual increases in Ocean Heat Content (OHC), sometimes expressed in mind-boggling terms such as 10²² joules per year (see Fig.1). While this may sound alarming [1,2], when converted to flux, it represents less than 1 W/m², a mere 0.6% of the average 160 W/m² of absorbed solar energy at the surface. All the rest is via evaporation, convection and ultimately by radiation sent back to space after globally being redistributed by wind and currents.

Although longwave *back-radiation* from the atmosphere penetrates only a few micrometers into ocean water, GHG-induced atmospheric warming will affect the ocean's top layer ($\sim 50-100$ m thick) by affecting its cooling. Below this layer, temperatures drop rapidly, and any excess heat is stored in deeper ocean layers where it remains for centuries due to poor conductivity and stable stratification.

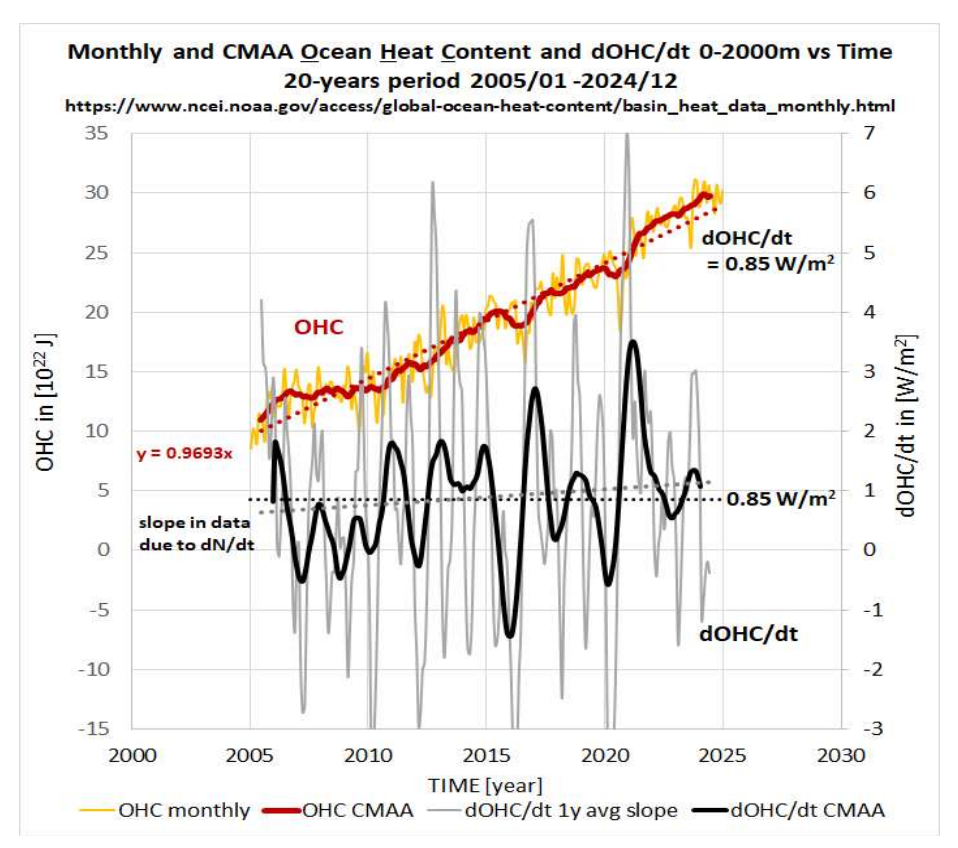


Fig. 1. Ocean Heat Content (OHC) anomaly from 0–2000 meters over time, shown as 3-month and annual moving averages (CMAA), along with their time derivatives. Notable are the relatively large variations, likely reflecting the influence of El Niño events. The average radiative imbalance at the top of the atmosphere (TOA), estimated at 0.85 W/m², corresponds approximately to the midpoint of the time series (around 2015). Data: https://www.ncei.noaa.gov/access/global-ocean-heat-content/basin heat data.html [7].

This raises the question: Why would extra GHGs that have only a limited effect on the 99.4% of the outgoing flux, have affected this 0.6% residue during a couple of decennia in such a way that we should be scared about all that "warming in the pipeline" as Hansen et al. [2] are warning us for? In the following sections, we examine data showing that observed trends in the radiation imbalance and OHC are better explained by the internal dynamics of the Earth's thermal system and natural forcings such as from increasing solar radiation, rather than solely by GHG emissions.

2. Climate balance in perspective

2.1. The ideal picture

A thermal system, such as a pot of water on a stove, reaches equilibrium when energy input matches energy loss. Analogously, Earth's thermal system absorbs shortwave (SW) solar radiation and emits longwave (LW) radiation. The average incoming solar flux at the top of the atmosphere is about 340 W/m², but due to Earth's albedo of 0.3, only about 240 W/m² enters the climate system. Although just 160 W/m² is actually absorbed at the surface, that SW_{IN}-flux determines the system's temperature, characterized by the averaged surface temperature T_S . This is reached when the cooling flux LW_{OUT} sent to space equals the influx from the Sun SW_{IN}, resulting in a constant climate with $dT_S/dt = 0$.

In fact, our cooling is realized through the transfer of heat from the surface to space, by a combination of long-wavelength (LW) radiation, convection and latent heat by evaporation of water. During its path through the atmosphere, that integral flux is finally all transferred into radiation by GHGs, mainly water vapor and CO₂. That radiation leaves our climate system to space as LW_{OUT} because there are no thermal flows possible anymore at TOA. We can forget here about

the details of the transfer processes involved as changes in our climate's parameters are relatively small *i.e.*, in the order of 1% per century. Accordingly, they can all be linearized in a first-order approach as in the following analyses.

The dynamics of our climate balance is illustrated in Fig.2a using a resistor-capacitor (RC) circuit: the heat capacity (C) of the climate system is charged by an incoming solar flux (SW_{IN}) and discharges via a resistor (R), which represents all combined heat loss processes (LW radiation, convection and evaporation). The system reaches equilibrium when incoming SW_{IN} and outgoing LW_{OUT} fluxes match *i.e.*, when the radiation imbalance $N = (SW_{IN} - LW_{OUT}) = 0$. Climate's equilibrium surface temperature T₀, is then set by SW_{IN} and R.

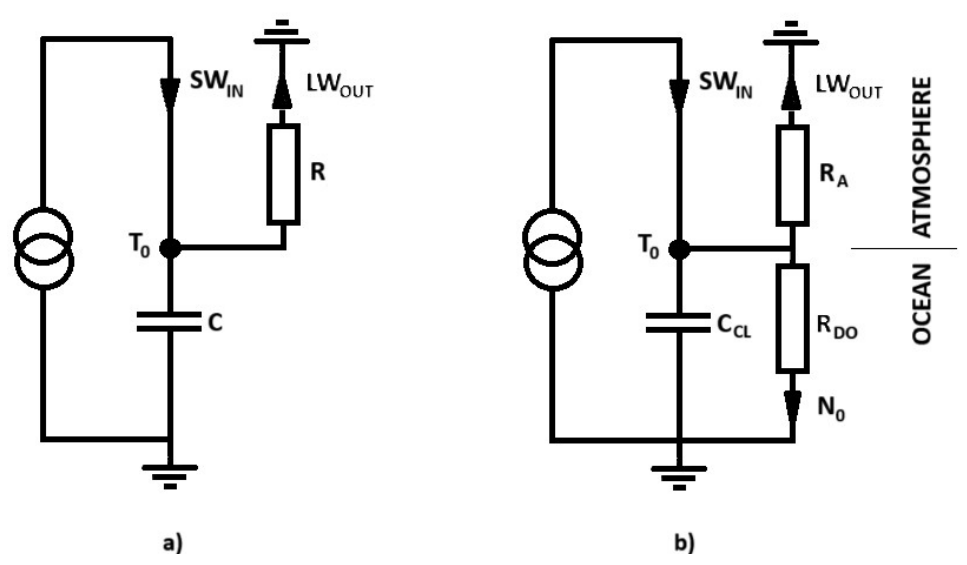


Fig.2. Schematic thermal circuit for our Earth' climate system, for illustration purposes only:

- a) In its most rudimentary form consisting of a heat capacitor C shunted by a resistor R coupled to a source with constant flux SW_{IN} .
- b) As a more realistic circuit where the heat capacity of our climate C_{CL} is separated from the rest of the Earth' (almost infinite) heat capacity and where a small part N_0 of the incoming flux is "leaking" from the climate system through the resistor R_{DO} to the deep ocean layers. R_{DO} is much larger than the resistance of the atmosphere R_A as N_0 is less than 0.6% of SW_{IN} (see Section 2.3)

Growing concentrations of GHGs increase the atmospheric resistance R to outgoing radiation, which upsets this balance. It is the background to the *Anthropogenic Global Warming* (AGW) hypothesis, promoted by the *International Panel on Climate Change* (IPCC) as the fundamental driver behind the observed warming since the beginning of the industrial era [8]. But, also changes in SW_{IN} due to for instance clouds will have similar effect on the imbalance N, thus inducing a change in temperature necessary to regain balance. For a step-wise offset Δ N at t = 0, between incoming and outgoing radiation forcing the average temperature T₀ to change to a new equilibrium (T₀ + Δ T), the respective time-paths for surface temperature T(t) and radiation imbalance N(t) for t > 0 are given by:

$$T(t) = T_0 + \Delta T \left(1 - exp(-t/\tau) \right) \tag{1a}$$

$$N(t) = \Delta N \left(exp(-t/\tau) \right) \tag{1b}$$

where $\tau = RC$ represents the relaxation time of the thermal system. For the new equilibrium temperature $(T_0 + \Delta T)$ at $t \to \infty$, we can couple ΔT to ΔN according to:

$$\lambda \, \Delta T = \Delta N \tag{2}$$

Science of Climate Change

where λ is called a *feedback* parameter. Its inverse, $\xi = 1/\lambda$ is our system's *climate sensitivity* relating the ultimate temperature change ΔT to the original disturbance in the energy balance ΔN . The higher ξ , the larger the temperature's reaction to a certain disturbance of the imbalance as the temperature at the surface "feeds" LW_{OUT} in restoring its balance. Also, the more difficult the transfer from the surface to space, the longer it takes to restore the balance. In case of extra heating by the Sun, or reduced cooling by extra CO₂, the amount of energy fed to this thermal system to restore balance, equals τ ΔN . The amount of heat necessary to increase the temperature equals C ΔT , yielding the important relation:

$$\tau = \frac{C}{\lambda} = \xi C \tag{3}$$

As the heat capacity of our climate system can be considered a given, the climate sensitivity scales with the relaxation time of our climate to disturbances. The relaxation time can a.o. be inferred from the various radiation components as measured at TOA by the CERES-program [9], as shown in Fig.3 with *Centered Moving Annual Averages* (CMAA) to remove cyclical/seasonal variation in the radiation components. The strong signal modulation with *peak-to-peak* times of roughly 3 years, must be indicative for the value of τ . This is far less than the 10 to 15 years for τ as the consequence of IPCC's high climate sensitivity [8], or the even longer times as claimed by Hansen *et al* [2]. If those would be the reaction time of our climate to disturbances, the observed large variations in the radiation imbalance data as shown in Fig.3 would be completely flattened out.

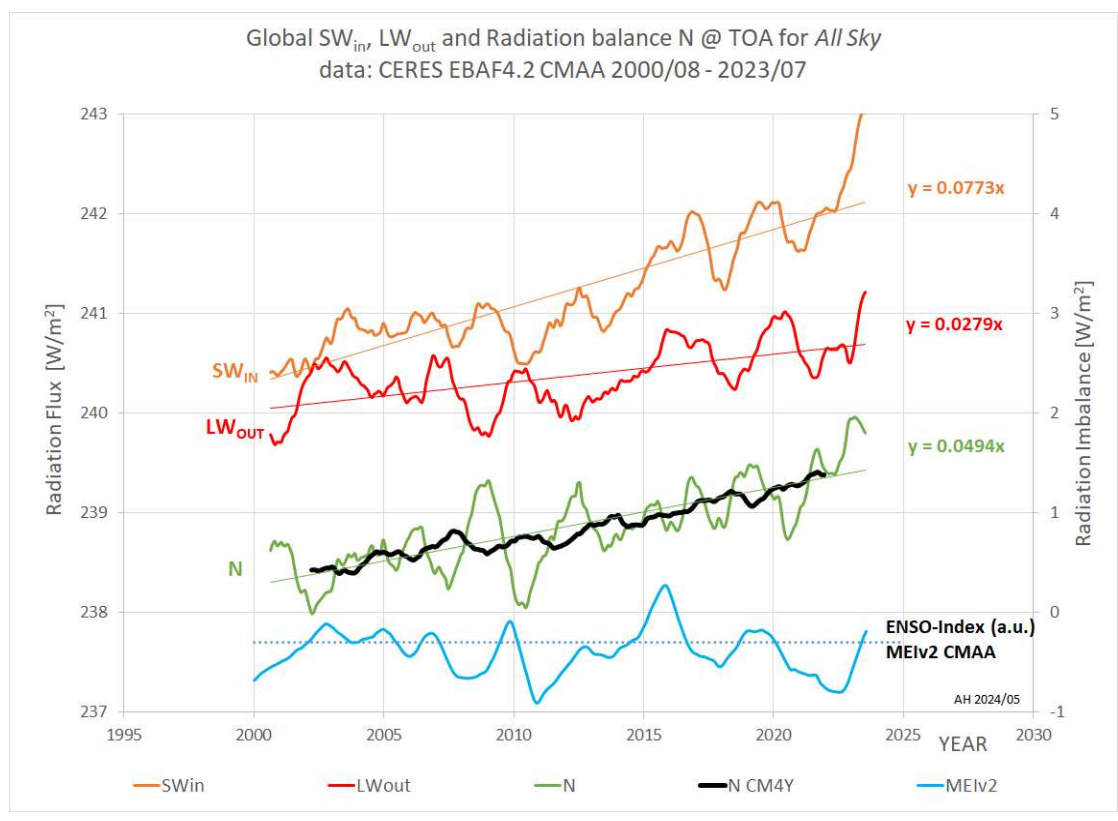


Fig. 3. Centered Moving Annual Averages (CMAA) of the measured radiation components at the top of the atmosphere (TOA): incoming shortwave radiation SW_{IN}, outgoing longwave radiation LW_{OUT}, and their difference, the radiation imbalance N. Linear trends are indicated. For the radiation imbalance N, a 4-year moving average (CM4Y) is also shown, highlighting the effect of a 3–5 years climate relaxation time. In contrast, filtering with a longer time constant (10–15 years), as assumed under the Anthropogenic Global Warming (AGW) hypothesis, would largely suppress these variations. The ENSO MEIv2 index (as CMAA) is included to illustrate the strength of El Niño, which is primarily responsible for large fluctuations in cloud cover and, consequently, in radiation. Data sources: https://ceres.larc.nasa.gov/data [9] and https://ceres.larc.nasa.gov/data [9] and https://psl.noaa.gov/enso/mei/ [10]

2.2. Estimating our climates thermal capacity C_{CL}

The rather fast responses of our climate indicates that the thermal capacity of our climate must be much less than the capacity of the entire *Earth thermal system*. This climate heat capacity C_{CL} depends on how sunlight is being absorbed, how that heat is transferred to the atmosphere and which part of it is being stored in either land or ocean.

At continental land-area, sunlight is absorbed only at the very surface where the generated heat is also in direct contact with the atmosphere. Seasonal temperature variations don't penetrate more that 1 to 2 meters deep in average and as a consequence, storage of heat is relatively small. Sunlight can penetrate pure water to several hundred meters deep, but in practice, penetration in the oceans is limited by scattering and absorption of organic and inorganic material. A good indication is the depth of the *euphotic* zone where algae and phytoplankton live, which need light to grow. In clear tropical waters where most of the sunlight hits our planet, this zone is 80 to 100 m deep [12].

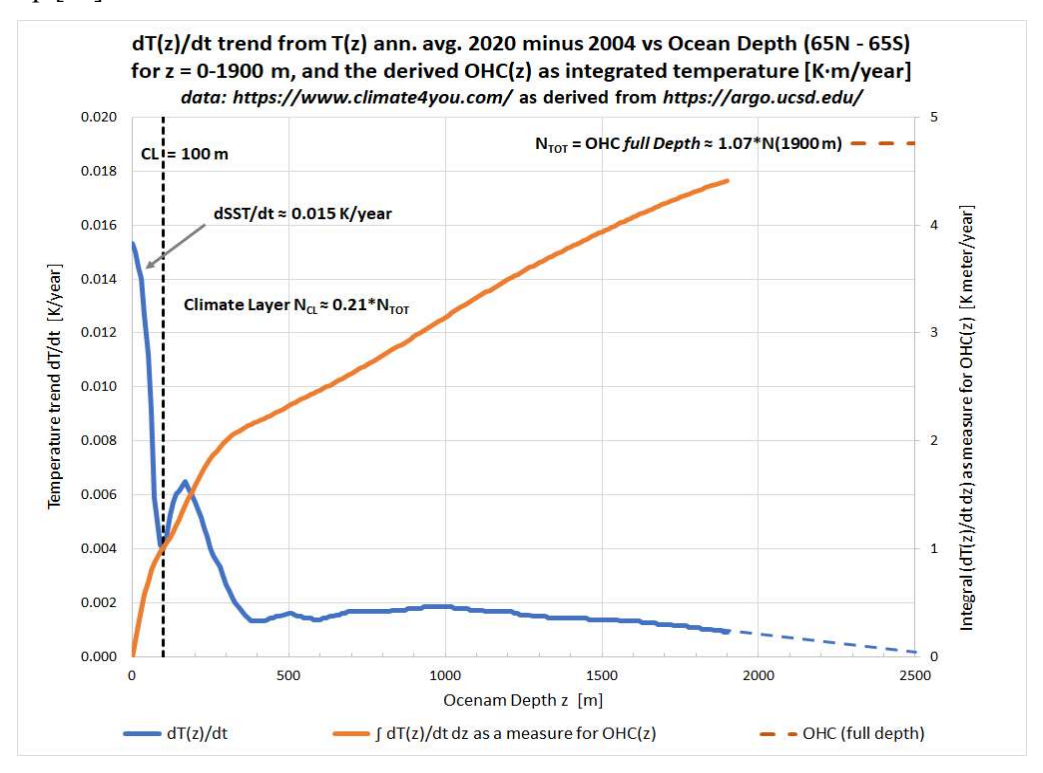


Fig. 4. Average temperature trend dT(z)/dt (blue) between 2004 and 2020 as a function of depth (0-1900 meters), for oceans between 65°S and 65 N. The surface temperature trend dSST/dt ≈ 0.015 K/year. The change in Ocean Heat Content (OHC) as a function of depth (orange) is obtained by integrating dT(z)/dt. The OHC over the full depth is estimated by extrapolation of dT(z)/dt below 1500 m. The temperature trend reveals a clear separation between the upper ocean (the "climate layer") and the deeper ocean. The climate layer is roughly 100 meters thick and stores about 20% of the total OHC. Temperature profile taken from https://www.climate4you.com/ (oceans) [14], based on https://argo.ucsd.edu/ [6]

The equivalent thermal capacity of our oceans per unit area must therefore be much larger than that of land. As the equivalent heat capacity of our atmosphere equals only a few meters of water, this absorption zone of our oceans that also cover over 70% of the Earth's surface, is in first-order a good indicator for our climate's heat capacity $C_{\rm CL}$.

Another important factor in our climate's heat capacity is how this ocean layer of absorbed heat is in contact with the atmosphere. Tides, wind, waves and convection continuously mix the top-layer of our oceans, by which heat is easily exchanged with the atmosphere. This *mixed-layer* is typically in the order of 25 - 100 m, dependent on season, latitude and on the definition of "well-mixed" [13]. Below this ~100 m thick top-layer, where hardly any light is being absorbed and the

mixing process has stopped, ocean temperatures drop quickly with depth. As the oceans' vertical temperature gradient at that depth doesn't support conductive nor convective heat flows going upward, climate processes at the surface will thus become isolated from the rest of the Earth' thermal system.

Figure 4 with the Change in Ocean Heat Content vs. Depth over the period 2004 - 2020 obtained via the ARGO-floats [6,14], offers a good indication for the average climate capacity C_{CL} . It shows the top layer with a high surface temperature change according to the observed global warming rate of about 0.015 K/year, and a steep cut off at about 100 m depth in line with the explanation above. Below the top layer, temperature effects are small and difficult to interpret, probably due to averaging over all kinds of temperature/depth profiles in the various oceans ranging from Tropical- to Polar regions.

A 100 m thick top-layer can be attributed to a climate heat capacity $C_{CL} \approx 13$ Wyear/m²/K. That is consistent with a climate relaxation time $\tau \approx 4$ years in combination with the *Planck feedback parameter* $\lambda_{PL} = -3.3$ W/m²/K according to relation (3): $\lambda_{PL} = -C_{CL}/\tau$ [4] (by convention λ_{PL} has a negative value, but $\lambda = 1/\xi$ in the formulas applied here, is regarded as a positive parameter).

The split between top-layer and rest of the ocean looks physically visible in Fig.4, but in fact, C_{CL} is no more than an "effective" climate heat capacity. Schwartz [5] calculates this effective heat capacity in a different way from a regression of OHC at various depths versus T_S . He concludes to a thermal capacity $C_{CL} = 14 \pm 6$ Wyear/m²/K, equivalent to 110 ± 50 m thick climate layer. The relaxation time of 5 ± 1 years is derived from the autocorrelation of global mean sea surface temperatures. Taken together, he concludes from applying (3), to a climate sensitivity of 0.30 ± 0.14 K/W/m², in essence equal to the inverse of $-\lambda_{PL}$ as the outcome of [4]. Margins encompass the $C_{CL} = 13$ Wyear/m²/K and $\tau = 4$ years as above, so we stick here to those values to remain consistent with earlier assessments [4].

A final remark on the heat involved in melting processes. Snow and ice increase the effective heat capacity of our climate as heat stored in this phase-transition cannot add anymore to warming. Processes like melting and freezing, occur at the atmosphere-surface interface and must be regarded as normal phenomena in our climate's natural reaction to warming or cooling. Therefore, they are supposed to be intrinsic to the "normal" climate sensitivity $\xi = 1/\lambda$.

2.3. A more realistic view on our climate's equilibrium and the radiation balance

In case of a "perfect" equilibrium (N=0, $dT_s/dt=0$), all of the absorbed sunlight up to about 100 m deep, has to leave on the ocean-atmosphere interface again. However, deep oceans are still very cold with a stable, negative temperature gradient towards the bottom. This gradient will anyhow push some of the absorbed heat downwards. Therefore, even at a climate equilibrium with $dT_s/dt=0$, we will observe N>0. With the large heat capacity of the total ocean volume, that situation will not change easily, as it takes about 500 years with today's $N\approx +1$ W/m² to raise its average temperature just 1°C.

The Earth's climate system can thus be regarded as a subset of the total *Earth's thermal system* (ETS) responding to different relaxation times. The climate relaxes to a new equilibrium within 3-5 years, while the deeper oceans operate on multidecadal or even longer timescales, related to their respective thermal capacities C for the ETS, and C_{CL} for the climate system.

The ratio C/C_{CL} must be large. A first, too large estimate would be about 45 between the 4.5 km depth in average for our oceans and the 100 m top-layer of the oceans that interact in the climate processes with the atmosphere. The inner core of the Earth however, is still hot. This heat is flowing upwards to the surface where it is assumed to be somewhat less than 0.1 W/m² [11]. The heat capacity of the ETS must therefore be limited to the layer above the depth where this upward heat flow equals the downward flow from the absorbed sunlight. The OHC-data hint to a depth of the ETS-capacity somewhere between 1000 and 2000 m, with an ETS-relaxation time 10-20x the relaxation time τ of our climate *i.e.*, about 40 to 80 years.

Science of Climate Change

This split up between the climate system and the Earth' thermal system has been expressed in the circuit-scheme of Fig.2b where a large resistor is added not only to make the separation, but also the connection between these two thermal systems visible. Any surplus in the radiation imbalance N, goes partly into warming of the climate capacity C_{CL} , which we experience as *global warming*. The remaining part, the flux N_0 , "leaks" through the large resistor R_{DO} into the much larger heat capacity of the rest of the ETS. From the heat fluxes through both media (1 vs 240 W/m²) we must conclude that $R_{DO} >> R_A$. Therefore, this decoupling doesn't make any difference for the surface temperature's set-point. The dynamics of the two thermal systems characterized by $\tau = R_A C_{CL}$ for our climate, and $R_A C$ for the ETS however, are completely different.

3. The "virtual balance" No in the balancing act of our climate

The heat flux N_0 , which leaks into the ocean's deeper layers (Section 2.3), does not contribute to the surface temperature and, by extension, to what we define as "climate." Still, it reflects a persistent offset in the Earth's radiation balance, even when surface temperatures appear stable *i.e.*, $dT_s/dt = 0$. This offset likely arises from slow changes in how heat is redistributed, either between top and bottom of the oceans and/or between Equator and Poles (see Section 1). Though part of the Earth's overall thermal system, N_0 acts as a *virtual balance* in the climate subsystem because it doesn't directly impact surface temperatures. This suggests that much of the observed increase in *Ocean Heat Content* isn't necessarily linked to changes in GHGs, as assumed in the AGW-hypothesis. Moreover, N_0 likely varies over time due to evolving wind patterns, changing ocean currents, or even local geothermal fluctuations [11].

This concept of a virtual balance lets us rethink the dynamics of our climate system under influence of an external forcing F(t) such as from extra GHGs and/or an increase in Solar flux. The driving force to change the surface temperature in order to restore balance is proportional to the deviation from equilibrium. By this concept, we can now separate the dynamics of the climate system from the much slower reacting Earth thermal system by considering deviations from that *virtual equilibrium* expressed as $(N(t) - N_0(t))$, by the following relation for disturbances of an equilibrium system:

$$\frac{d(N(t) - N_0(t))}{dt} = \frac{dF(t)}{dt} - \frac{N(t) - N_0(t)}{\tau} \tag{4}$$

In the absence of external forcings (dF/dt = 0), N(t) relaxes back to $N_0(t)$ exponentially with a characteristic time τ according to (1b).

The driving force to restore equilibrium $(N(t) - N_0(t))$ is coupled to the surface temperature as in (2). So, the surface temperature T_S that is applied here as characteristic for our climate, will rise according to $(N(t) - N_0(t))$ divided by the climate heat-capacity C_{CL} :

$$\frac{dT_S(t)}{dt} = \frac{N(t) - N_0(t)}{C_{CI}} \tag{5}$$

Here we assume a constant C_{CL} . If not, for example due to slow changes in the ocean top-layer, the term $T_S dC_{CL}/dt$ that we then have missed to account for in (5), will automatically be incorporated in $N_0(t)$. By rearranging (4) and applying (3) with $\lambda = C_{CL}/\tau$, we can now rewrite (4) as:

$$\frac{dN}{dt} = \frac{dN_0}{dt} + \frac{dF}{dt} - \lambda \frac{dT_S}{dt} \tag{6}$$

If $N_0(t)$ itself changes over time, dN_0/dt in (4) becomes indistinguishable from external forcings and should be included in the trend of total forcings $dF_{TOT}/dt = dF/dt + dN_0/dt$, thus creating a well-known relation in climate literature:

$$\frac{dN}{dt} = \frac{dF_{TOT}}{dt} - \lambda \frac{dT_S}{dt} \tag{7}$$

Science of Climate Change

In (6) and (7), time dependencies have been left out as these relations have only practical use in analyzing climate data when considering longer term trends. The trend indication dX/dt for a parameter X as applied here, stands in fact for the change ΔX over a period $\Delta t >> \tau$. In climate literature, one often uses (7) in this Δ -format:

$$\lambda \Delta T_S = \Delta F_{TOT} - \Delta N \tag{8}$$

to determine the climate sensitivity $\xi = 1/\lambda$ from the sum of all known forcings in ΔF_{TOT} , the observed changes in imbalance ΔN and average temperature ΔT , over a certain period [15]. Calculation with (8) might underestimate the value for λ as one easily "forgets" the positive contribution ΔN_0 in ΔF_{TOT} .

4. Available data used in the analysis

4.1. Radiation data at TOA

The most comprehensive radiation dataset is NASA's CERES-EBAF v4.2 [9]. For our analysis, we use monthly SW_{IN} , LW_{OUT} , and N data from 2000 onward, processed as *Centered Moving Annual Averages* (CMAA) to eliminate seasonal/cyclical effects and highlight long-term trends. These trends as shown in Fig.3 in units of [W/m²/year], are for the 23 years full 12 months period 2000/8 - 2023/7.

Satellite-based absolute radiation measurements with an uncertainty of about 3–5 W/m² per channel, are unfit to directly detect a radiation imbalance of about 1 W/m², as reported by NASA in Fig.3. Actually, this imbalance is calibrated using the time derivative of *Ocean Heat Content* dOHC/dt, as explained in Section 4.2. While the absolute values may be uncertain, the anomalies and trends in the CERES data are considered as being reliable, thanks to regular *in situ* calibration of the satellite sensors.

4.2. Ocean Heat Content (OHC) data

The current radiation imbalance $N(t) \approx 0.85~W/m^2$, is estimated from dOHC/dt shown in Fig.1 [7]. Ocean Heat Content data are derived from vertical temperature measurements across the global oceans, collected by the ARGO float network [6]: a system of autonomous buoys that cycle to depths of ~2000 meters, measuring parameters like water temperature as they descend and ascend.

Figure 3 (along with Fig.1) reveals that short-term fluctuations in the TOA radiation imbalance don't always align with OHC trends. For example, the peak and dip around 2016 seen in OHC are not reflected in the TOA radiation imbalance data. However, those variations do appear in the incoming solar radiation SW_{IN}, which directly influences ocean heating. This correlation supports the inclusion of the term dN_0/dt in (6), representing the heat flux into deeper ocean layers.

Figure 4 shows that heat continues to flow below 1900 meters, although modestly. A simple linear extrapolation suggests total OHC is about 1.10 times the measured OHC down to 1900 m. This correction factor (1.07) is applied to values derived from OHC, such as the calibrated absolute radiation imbalance in the CERES dataset, resulting in an updated estimate: $N \approx 0.94~W/m^2$. It does not apply to $dN/dt \approx 0.049~W/m^2/year$ however, as it comes directly from NASA's radiation measurements at TOA.

Figure 4 also shows that about 20% of the OHC change occurs in the top 100 meters of the ocean. This surface layer interacts strongly with the atmosphere and is therefore, not included in N_0 , the flux into the deeper ocean. The energy flux absorbed in this *climate layer* $N_{CL} = (N - N_0) = C_{CL} dT_s/dt$, as required by conservation of energy. From Fig.4 we estimate a value for $N_{CL} \approx 0.20*1.1*0.85 \approx 0.19$ W/m², which implies $N_0 \approx 0.75$ W/m² (averaged over 2004 – 2023). This value immediately shows, that N_0 is not near the thermal flux to the bottom as a result of the much warmer top-layer. The maximum in the average temperature gradient towards the bottom

of the oceans of about 0.06 K/m as obtained from the ARGO-data, is found just under that top-layer. With a thermal conductivity coefficient of salty sea water around 15 °C of 0.58 W/K/m, we can only explain 0.035 W/m² i.e., a contribution of just 5% of the energy flux that heats the lower part of the oceans. So, most of that heat must come from absorbed solar radiation below the climate layer.

4.3. Temperature trends

To apply (6), we need a reliable estimate of the surface temperature trend. While many datasets exist, each with strengths and limitations [16], we focus in this paper on two key sources. The first is the HadCRUTv5 series from the UK Met Office [17], which shows a relatively high trend of 0.023 K/year over the 2000–2023 period. This dataset is based on a mix of ground stations and buoys. Its global average is obtained through interpolation and homogenization algorithms. However, because many land-based stations are located near urban areas and airports, these records may be affected by local warming biases [19].

The second dataset is UAH-TLT from the Univ. of Alabama Earth System Science Center [18], based on satellite observations of microwave emissions from the *Lower Troposphere* (LT). It provides near-complete global coverage in a 1°x1° grid and shows a lower trend of 0.015 K/year for this period.

Figure 4 shows that the sea surface temperature (SST) trend derived from ARGO data is approximately 0.015 K/year, closely matching the 0.0135 K/year trend in the ocean-only portion of the UAH-TLT dataset. In contrast, the HadSSTv4 dataset [20] (assumingly the ocean component of HadCRUTv5) shows a higher SST trend of 0.019 K/year, indicating a significant discrepancy. We don't know what causes this unexpected difference, but it is noteworthy since the ARGO floats are presumably part of the buoy network used in constructing the HadSSTv4 series.

4.4. Greenhouse gas forcings

Since the start of CERES measurements in 2000, the concentration of greenhouse gases (GHGs), especially CO₂, has increased significantly. These concentrations have been reliably monitored since the early 1960s through daily observations, and the quality of these data is widely accepted.

Figure 5 shows the total atmospheric concentration of all *well-mixed* Greenhouse gasses, such as for instance Methane (CH₄), expressed as CO₂-equivalent by applying relative GHG-strengths [21]. For simplicity, we refer to this further on as "CO₂". Because CO₂-forcing is proportional to the logarithm of its concentration, a logarithmic scale is used on the vertical-axis. This reveals that CO₂ concentrations have followed a near-perfect exponential trend since the mid-1970s. Consequently, the forcing trend from GHGs (dF_{GHG}/dt) has remained approximately *constant* for over 4 decades, and it's unlikely to increase significantly. Net-zero initiatives in developed countries are slowing emission-growth, and global population, another major driver, is expected to stabilize later this century.

The actual forcing-trend dF_{GHG}/dt depends on the value for the forcing from doubling the CO_2 -concentration F_{2xCO2} commonly expressed as:

$$\frac{dF_{GHG}}{dt} = F_{2xCO_2} \frac{d}{dt} (\ln[CO_2]) / \ln(2)$$
(9)

According to NASA's AGGI database [21] $dF_{GHG}/dt \approx 0.035 \text{ W/m}^2/\text{year}$, indicating $F_{2xCO2} = 3.7 \text{ W/m}^2$. IPCC, in its AR6 report [8], uses a slightly higher $RF_{2xCO2} = 3.9 \pm 0.5 \text{ W/m}^2$, leading to a trend of $0.037 \text{ W/m}^2/\text{year}$.

However, applied forcing strengths depend on the definition of radiative forcing (RF). The IPCC defines its RF at the *Top of the Troposphere* (TOT) where thermal fluxes are still present, whereas in (4)-(7) the forcing trends used, refer to the *Top of the Atmosphere* (TOA). This matters a lot,

Science of Climate Change

as IPCC's definition excludes cooling effects of increasing GHGs in the *Stratosphere*, leading to systematically higher forcing values that may overstate surface warming considerably.

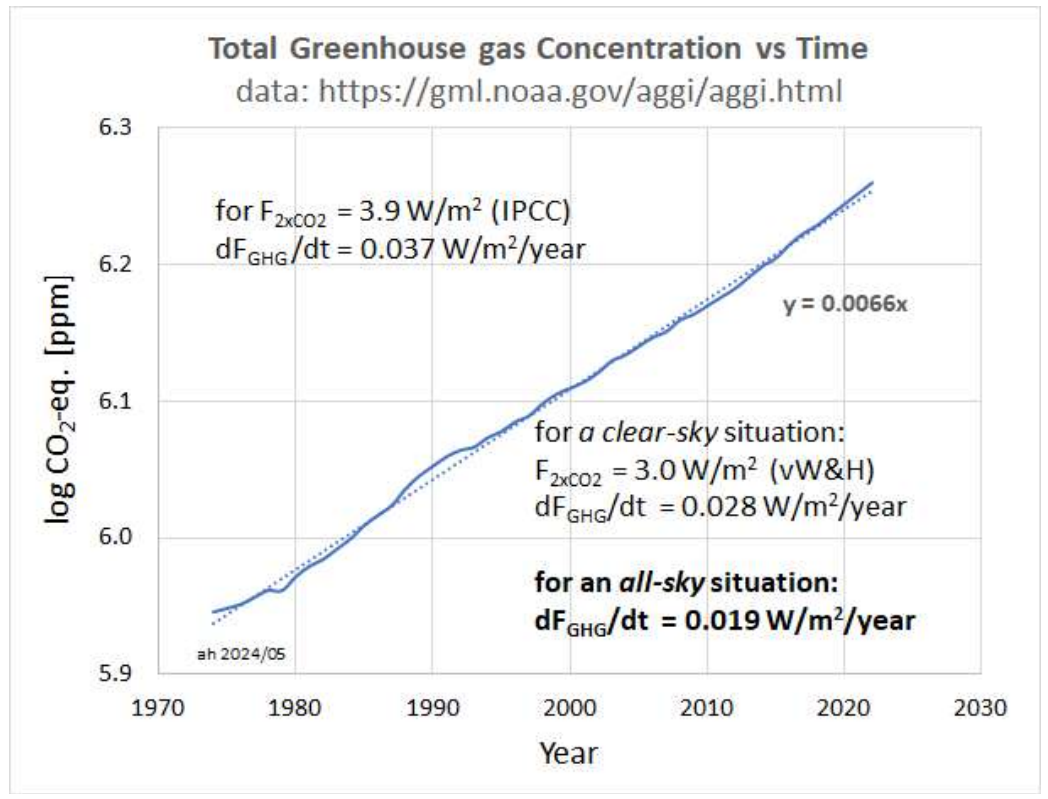


Fig. 5 Time evolution of the CO₂-equivalent concentration of all greenhouse gases (GHGs), based on data from [21]. The slope of this logarithmic plot indicates an almost constant radiative forcing trend over the past 40 years, in accordance with (9). With IPCC-AR6 "most likely" value of $RF_{2xCO2} \approx 3.9 \ W/m^2[8]$, it implies a GHG forcing trend $dF_{GHG}/dt = 0.037 \ W/m^2/year$ over the entire period. Using the recent "clear-sky" calculations by van Wijngaarden and Happer [22], the trend is $\sim 0.028 \ W/m^2/year$. Accounting for the average $\sim 2/3$ cloud cover ("all-sky" conditions), the effective forcing trend is then significantly lowered to: $dF_{GHG}/dt \approx 0.019 \ W/m^2/year$ [25] (see the text for details).

For comparison, Van Wijngaarden & Happer [22] report $F_{2xCO2} = 3.0 \text{ W/m}^2$ at TOA based on thorough radiative transfer calculations. For RF according to the IPCC definition at TOT, they calculate 5.5 W/m², illustrating the significant cooling from GHGs in the Stratosphere. Rentsch [23], reports an experimental value of 2.65 W/m², based on analyzing 17 years of satellite based spectroscopic data.

These non-IPCC F_{2xCO2} values are calculated/established under *clear-sky* conditions. But, on average, two-thirds of the Earth is covered by clouds, strongly modulating GHG effects. Clouds reduce outgoing radiative fluxes: only ~1/3 originates from the surface and fully "feels" GHG forcing over the entire atmospheric column. The other ~2/3 comes from *Top of Clouds* (TOC) levels. TOC radiation is not only lower (due to lower TOC-temperatures) but also traverses a thinner atmospheric layer, reducing the greenhouse effect. Although CO_2 is more effective above clouds where water vapor as a major overlapping absorber is nearly absent, the negative contribution due to the large cooling effect of GHGs in the Stratosphere however, remains constant by absence of clouds at those heights.

To estimate the net *all-sky* forcing, we can adjust *clear-sky* results using a "*Venetian blinds*" model [25] and *MODTRAN* simulations [24] applying TOC-temperature and -altitude from satellite data. This yields $F_{2xCO2} \le 2.0 \text{ W/m}^2$, about half the value used in IPCC AR6 [8].

Although IPCC's RF_{2xCO2} = 3.9 W/m^2 is defined at TOT, it most probably represents a real *all-sky* value, as it comes from GCM simulations that include cloud effects. Comparing it to the 5.5 W/m^2 as calculated for the *clear-sky* TOT-situation [22], yields a ratio of 0.71. Applying this ratio to the *clear-sky* calculated $3.0 \text{ W/m}^2/\text{K}$ at TOA, indicates an *all-sky* $F_{2xCO2} \approx 2.1 \text{ W/m}^2$. This aligns well

with the 2.0 W/m² estimate from the *Venetian blinds* model [25], thus giving confidence in the *all-sky* forcing trend as derived via (9): $dF_{GHG}/dt \approx 0.019 \text{ W/m}^2/\text{year}$.

5. Climate change in perspective

5.1. Splitting the Total Forcing Trend

In (7) all possible forcings trends at TOA including GHG-contributions dF_{GHG}/dt , were combined into a single term dF_{TOT}/dt . Since GHGs primarily act in the LW-channel, it is logical to split up the total forcing into: $dF_{TOT}/dt = dF_{NA}/dt + dF_{GHG}/dt$. Here the subscript "NA" refers to "natural" and/or "non-anthropogenic" contributions. This includes forcings in the SW-channel as *e.g.* from aerosols, changes in the Earth' *albedo*, either from changes in cloudiness or changes in the surface reflection, and changes in N_0 , the heat disappearing into the deep ocean. Although clouds affect both SW and LW radiation, their "net" radiative impact described as the *Cloud Radiative Effect* (CRE) can be reasonably well attributed to the SW-channel only. We can therefore split up the total forcing even a step further into $dF_{TOT}/dt = dN_0/dt + dF_{SW}/dt + dF_{GHG}/dt$. Later on, in Section 8, we will discuss how dF_{SW}/dt can be fully linked to the large observed incoming solar trend dSW_{IN}/dt as shown in Fig.3. For now, it is just the trend of an unknown forcing in the SW-channel.

For the analysis we can rewrite (6) as:

$$\frac{dN}{dt} = \frac{dN_0}{dt} + \frac{dF_{SW}}{dt} + \frac{dF_{GHG}}{dt} - \lambda \frac{dT_S}{dt}$$
 (10)

We could have kept dN_0/dt as a "natural" forcing trend, "invisibly" included into dF_{NA}/dt . Its explicit treatment will prove important later.

5.2. Testing the AGW-GHG-only hypothesis

Suppose, we had no other forcings in our climate than those from GHGs as is basically assumed in IPCC's AGW-hypothesis. That would imply $dSW_{IN}/dt = dN_0/dt = 0$ and (10) simplifies to:

$$\frac{dN}{dt} = \frac{dF_{GHG}}{dt} - \lambda \frac{dT_S}{dt} \tag{11}$$

Since at present, $dT_s/dt > 0$ and $\lambda = C_{CL}/\tau > 0$ (by definition) we know for sure that according to (11): $dN/dt < dF_{GHG}/dt$. This is also to be expected in a stable system where the "effect" of a disturbance will be smaller than its "cause". The observed value for $dN/dt \approx +0.049 \text{ W/m}^2/\text{year}$ according to the CERES-data (Fig.3) however, even exceeds the highest estimates for $dF_{GHG}/dt \approx 0.019 - 0.037 \text{ W/m}^2/\text{year}$ (see Section 4.4 for the range). Even IPCC's large value for the trend in GHG-forcing cannot explain the trend in the observed radiation imbalance, at all. It directly falsifies the AGW-hypothesis with GHGs as the sole drivers of Global Warming.

5.3. The onset of Global Warming and the forcing dynamics at that time

There is another challenge to the "GHG-only" scenario. At some point in the mid-1970s, the global cooling trend during the previous decennia reversed, and the modern warming period began. At that "turning" point in temperature at $t = \zeta$, we must have had: $dT_S(\zeta)/dt = 0$ and $d^2T_S(\zeta)/dt^2 = 0$. According to (5) $dT_S/dt = 0$ implies $N(\zeta) = N_0(\zeta)$, and $d^2T_S/dt^2 = 0$ requires: $dN(\zeta)/dt = dN_0(\zeta)/dt$.

With $C_{CL} > 0$, equation (11) delivers the important observation that: $dN(\zeta)/dt = dF_{GHG}(\zeta)/dt$.

Figure 5 clearly shows a $dF_{GHG}/dt > 0$ at that time. So, if the AGW-hypothesis is correct, warming began with a positive trend in the radiation imbalance $dN(\zeta)/dt > 0$. As dF_{GHG}/dt has been constant ever since, the rising temperature would have caused a declining imbalance $(d^2N/dt^2 < 0)$

Science of Climate Change

eventually leading to $dN/dt \rightarrow 0$ for $t >> \tau$. This would imply, 50 years later, a climate in a *steady state* where the temperature would track the constant trend in GHG-forcing according to $\lambda dT_S/dt = dF_{GHG}/dt$. As then dN/dt = 0, we would observe a constant offset in the radiation imbalance given by $N = \tau dF_{GHG}/dt \approx 0.08 - 0.16 \text{ W/m}^2$, depending on the choices for F_{2xCO2} and τ . Accordingly, $dLW_{OUT}/dt = 0$ at a constant solar input as assumed in the AGW-hypothesis.

This is nowhere near the observed imbalance $\sim 0.94~W/m^2$, its large non-zero trend dN/dt $\approx 0.049~W/m^2$ /year and dLW_{OUT}/dt $\approx 0.028~W/m^2$ /year. It might explain the need for the IPCC to increase F_{2xCO2} as much as possible, as well as to lengthen τ by increasing the climate sensitivity. But this introduces additional inconsistencies. Combining the observed imbalance and the high IPCC forcing trend, would indicate a relaxation time $\tau = N^*(dF_{GHG}/dt)^{-1} \approx 25~years$. If the imbalance began decreasing in the 1970s, it should even with this value have relaxed significantly by now to about 20% of its initial value $dN(\zeta)/dt = dF_{GHG}(\zeta)/dt$. Instead dN/dt as observed is still large, fully contradicting this expectation. Moreover, the AGW-GHG-only hypothesis can never explain the large dLW_{OUT}/dt as observed.

The corresponding climate thermal capacity C_{CL} would be $N*(dT_S/dt)^{-1} \approx 40$ - 60 Wyear/m²K, or equivalent to a *climate layer* of 300 - 450 meters thick. However, ARGO temperature-data show that seasonal variations don't penetrate much deeper than about 100 meters [14]. Below 200 meters, ocean temperatures are effectively decoupled from surface variations. That is consistent with the arguments in Section 2.4 about the parameters that determine the *climate layer* and the subsequent estimate for C_{CL} of about 13 Wyear/m²K *i.e.*, the heat capacity of a 100 m thick ocean layer.

5.4. Climate change and the important role of Solar Forcing

In Section 5.2 we derived the two key conditions that must have been met at the transition point between the global cooling- and global warming regimes: $N(\zeta) = N_0(\zeta)$, and $dN(\zeta)/dt = dN_0(\zeta)/dt$. Substituting those into (10) that still contains all these components, gives a remarkable equality:

$$\frac{dF_{SW}}{dt} + \frac{dF_{GHG}}{dt} = 0 ag{12}$$

This implies that at $t = \zeta$, the definitely positive forcing trend from GHGs was entirely offset by a negative trend in the forcing in the incoming solar channel *i.e.*, $dF_{SW}(\zeta)/dt \approx -0.019 \ W/m^2/year$, or even more negative depending on the choice for F_{2xCO2} . However, as shown in Fig.3, it is unambiguous that the current trend in incoming radiation $dSW_{IN}/dt >> 0$, indicating that today's $dF_{SW}/dt > 0$.

This leads us to conclude that the mid-1970s shift in climate change was not initiated by increasing GHG concentrations, but rather by a change in the trend of SW-channel forcings. During the preceding cooling period, rising CO₂ concentrations may have mitigated some of the cooling, but did not reverse it. Once the SW forcing trend turned positive, GHGs simply began to augment an already warming climate trend.

5.5. The (near) "steady state" character of current climate change.

Despite the ongoing changes in climate, the current state can be considered a "near" steady-state. The GHG forcing trend has been pretty constant for decades. Other forcings, primarily in the SW channel, are also likely to change slowly and can be approximated as having constant trends over decadal timescales. Similarly, despite yearly fluctuations, the surface temperature trend has remained fairly stable since 2000. This stability implies by the same logic as in Section 5.2, that dT_S/dt is (near) constant, and according to (5) that $(N-N_0)$ is (near) constant too. This allows for a large dN/dt as observed, but also indicates that $dN_0/dt \approx dN/dt$. From the OHC-data (Fig.4) we estimate that since $t = \zeta$ when $dN_0(\zeta)/dt = dN(\zeta)/dt$, dN_0/dt and dN/dt slowly developed to the present relation $dN_0/dt \approx 0.8*dN/dt$. Inserting this in (10) results in:

$$\lambda \frac{dT_S}{dt} \approx \frac{dF_{SW}}{dt} + \frac{dF_{GHG}}{dt} - 0.2 \frac{dN}{dt}$$
 (13)

The 0.2*dN/dt cannot be neglected as it indicates the growing divergence in the order of about 10 mW/m²/year. As a forcing, this is equivalent to a correction in the temperature trend of something like 3 - 10 mK/year, depending on the assumed climate sensitivity (see Section 6.1).

This analysis strengthens the conclusion that the increase in both N(t) and $N_0(t)$ are not a direct consequence of greenhouse gas emissions, but rather of enhanced forcing in the SW-channel. The alleged accelerations in N(t) that triggered this study [1], must therefore be attributed to natural variations in the SW-channel, not GHGs. This also explains why we didn't include dN_0/dt into the sum of forcing trends dF_{TOT}/dt in (10). If we had assumed a full *steady state* with $d(N-N_0)/dt=0$, we would have immediately noticed that (10) equals:

$$\lambda \frac{dT_S}{dt} = \frac{dF_{SW}}{dt} + \frac{dF_{GHG}}{dt} \tag{14}$$

A formula that we previously derived from a different perspective by perturbing the radiation fluxes in the SW- and LW-channels, going from one equilibrium to another. Begin and end state then both inherently satisfy the *steady state* condition $d(N-N_0)/dt=0$. It was shown that based on the *Planck feedback* definition $1/\lambda_{PL}=-\partial T_S/\partial N$, the feedback parameter in (14) must then be $\lambda=-\lambda_{PL}$ [4].

Equation (14) determines the temperature trend in our climate due to slow changing forcings with a constant trend in either the SW- or LW-channel. These can be attributed to GHGs, aerosols or changes in cloudiness. In case the imbalance $d(N-N_0)/dt$ isn't fully relaxed to zero, the small remaining imbalance will be absorbed in a slightly different estimate for dF_{SW}/dt , keeping (14) still practically applicable. Using the relation $\lambda = C_{CL}/\tau$, we can rewrite (14) linking this sum of "external" forcings $dF_{EXT}/dt = dF_{SW}/dt + dF_{GHG}/dt$ to the OHC-trend for the *climate layer*:

$$C_{CL}\frac{dT_S}{dt} = (N - N_0) = N_{CL} = \tau \frac{dF_{EXT}}{dt}$$
 (15)

The term $\tau dF_{EXT}/dt$ is the offset in the radiation imbalance N due to all external forcings F_{EXT} .

6. A comparative analysis of the data against different views on climate change

6.1. Input data-sets

In this section, we apply the relations as derived in amongst others Section 5, to explore two contrasting perspectives on three fundamental parameters governing climate change: climate sensitivity λ , temperature trend dT_S/dt and trend in GHG-forcing dF_{GHG}/dt .

The first set, based upon IPCC's views and further referred to as the "IPCC-set", consists of:

$$\lambda = \lambda_{AGW} = 1.1 \text{ W/m}^2/\text{K}, dT_S/dt = 0.023 \text{ K/year} \text{ and } dF_{GHG}/dt = 0.037 \text{ W/m}^2/\text{year}.$$

For the *Equilibrium Climate Sensitivity* (ECS), IPCC reports 3 °C with a "*likely*" range of 2.5 – 4 °C. Their *best estimate* corresponds to $\lambda_{AGW} = 1.3$ W/m²/K using ECS = RF_{2xCO2}/ λ_{AGW} . For the simplicity of maintaining a clean 3x ratio with λ_{PL} , we adopted the midpoint of the *likely* range, in line with CMIP6 ESM as referred to by the IPCC [8].

The second set, further referred to as the "NAT-set" consists of quite different numbers with:

$$\lambda = -\lambda_{PL} = 3.3 \text{ W/m}^2/\text{K}, \ dT_S/dt = 0.015 \text{ K/year, and } dF_{GHG}/dt = 0.019 \text{ W/m}^2/\text{year.}$$

Values originate from the analysis in [4], which initially also used IPCC's GHG-forcing trend ($dF_{GHG}/dt = 0.037 \text{ W/m}^2/\text{year}$). That choice led then to a large mismatch with the observed *clear-sky* dLW_{OUT}/dt, prompting the *all-sky* recalculation for F_{2xCO2} [25].

Science of Climate Change

A fixed climate relaxation time $\tau=4$ years is assumed for both sets. The consequence of IPCC's large climate sensitivity $1/\lambda_{AGW}$ is that with this constant τ , the heat capacity of our climate C_{CL} must become small. A shallow *climate layer* of about 30 meters is not very realistic, given the OHC-profile in Fig.4. To maintain consistency in the *IPCC-set* a longer relaxation time should be chosen ($\tau \approx 12$ years), or alternative combinations of C_{CL} and τ such that $C_{CL}/\tau = \lambda_{AGW}$. As earlier discussed, a 12 years relaxation time doesn't seem realistic. In discussing the calculated results in Section 6.1, we will address the possible impact of this choice where applicable.

6.2. Data comparison and sensitivity sets as applied in Table 1

For reference, Table 1 also includes a block of data derived from the observed OHC trends discussed in Section 5.2. Color-coding indicates which OHC-set parameters should be compared with the parameters calculated using (7) with $dF_{TOT}/dt = \lambda dT_S dt + dN/dt$ and (10), decomposing dF_{TOT}/dt into dF_{GHG}/dt , dF_{SW}/dt and dN_0/dt . Formulas used are indicated in the respective columns.

Climate sensitivity ξ , is generally expressed in its inverse as feedback parameter λ . It is by far the most controversial parameter and key differentiator between the two primary data sets. Their difference is so significant that exact values for the other parameters might be less critical. To illustrate how results depend on those parameters, we added to each climate sensitivity, also the temperature- and forcing trends of the other set. In this way we constructed 4 different sets. For the two primary sets, figures are shown in **bold** and for the two "hybrid combinations" in *italics*. Rows for these hybrids aren't colored in the table. They are not considered viable climate-scenarios but just added to make the sensitivity for certain parameter choices more visible.

Table 1. Summary of the radiation balance analysis for 4 scenarios. The two most relevant scenarios are the standard IPCC scenario (IPCC-set) and an alternative scenario (NAT-set) as described in the text. The primary input parameters include the inverse of the climate sensitivity λ , the trend in Greenhouse gas forcing dF_{GHG}/dt and the observed surface temperature trend dT_S/dt . Using these parameters, various related components were calculated based on eq.(7) & (10), and where possible, compared with values derived from the Ocean Heat Content analysis in Sections 3 & 4. In the (colored) rows belonging to the two key scenarios, values are shown in **bold**; in the other scenarios, values are italicized. Identical color-coding is used to visually link corresponding values from the radiation balance and OHC analyses.

	INPUT			$\lambda \Delta T = \Delta F_{TOT} - \Delta N$		DERIVED PARAMETERS				CHECK	AGW indicator
	λ [W/m²/K]	dF _{GHG} /dt [W/m²/y]	dΤ _s /dt [K/y]	$\lambda dT_s/dt$ [W/m²/y]	dF _{TOT} /dt [W/m²/y]	N ₀ [W/m ²]	dF _{NA} /dt [W/m²/y]	dN _o /dt [W/m²/y]	dF _{sw} /dt [W/m²/y]	dN/dt [W/m²/y]	$\Delta T_{GHG}/\Delta T$
	Assumed	Assumed	Measured	Calc	Calc	Calc	Calc	Assumed	$IPCC-AGW$ $dF_{SW}/dt = 0$	Calc	Calc
IPCC-set	1.1	0.037	0.023	0.026	0.075	0.83	0.038	0.039	-0.001	0.0494	1.44
		0.019	0.015	0.017	0.066	0.87	0.047	0.039	0.008	0.0494	1.14
			26		ä	3 30		"Near" Steady State	78	Alia - Alia	
NAT-set	3.3	0.037	0.023	0.077	0.127	0.63	0.090	0.039	0.051	0.0494	0.48
		0.019	0.015	0.050	0.099	0.74	0.080	0.039	0.041	0.0494	0.38
	Measured					2 50 0		20			
dN/dt	0.0494	$[W/m^2/y]$					Д	+	10		Q:
$\tau = C_{CL}/\lambda$	4	[y]		λdΤ	₫		dF _{NA} /dt	Stea	a _E	dN/dt + d	AT P
From	OHC-data de	erived		λdT _s /dt =	dF _{TOT} /dt	ح اا	/dt =	Steady State: $dN_0/dt \approx dN/dt$ rom OHC: $dN_0/dt \approx 0.79 dN/d$	dF _{Sw} /dt	/dt = dF _{GHG} /dt + dF _S + dN _O /dt - (N - N _O)/τ	$\Delta T_{GHG}/\Delta T = (dF_{GHG}/dt)/(\lambda dT_{S}/dt)$
N(1900m)	0.85	[W/m ²]			<u>o</u> .		g.	dN _o	<u>a</u>	at at	Œ.
N	0.94	[W/m ²]	1	- 2	N/N	ķ	or/e	/dt	N.	- N	¥_
N _{CL}	0.19	[W/m ²]]	°)/رد	<u>‡</u>	N - tÀdTg/dt	7	/dt ≈ 0.	<u>.</u>	- dt +	dt)/(
N _o	0.75	[W/m ²]		$(N - N_0)/\tau = N_{CL}/\tau$	dN/dt +λdT _S /dt	dt	dF _{ror} /dt - dF _{GHG} /dt	/dt = dN/dt = 0.79 dN/dt	= dF _{NA} /dt - dN _o /dt	$dF_{GHG}/dt + dF_{SW}/dt + dF_{GHG}/dt - (N - N_0)/\tau$	λdī
N _{cu} /τ	0.047	[W/m ² /y]		CI/4	/dt		P/ ⁵¹	N/d N/d	/dt	h/104	(dt)
N _{CL} /N _{TOT}	0.20			5520			+	# *		7	

6.3. Explaining/discussing the output parameters in Tabel 1

In this section, we systematically explain each column in Table 1 and relate them to the output derived from OHC data, as shown in Figures 1 and 4. For the radiation imbalance trend, we use the CERES-EBAF4.2 dataset, as numerically illustrated in Fig.3.

- $\lambda dT_S/dt$ expresses the climate response to the combined effect of all *forcings*. It is the warming of the *climate layer* through $\lambda dT_S/dt = N_{CL}/\tau$. In the *NAT-set*, using the *Planck feedback* parameter $-\lambda_{PL}$ this relationship is well satisfied. But in the *IPCC-set* using λ_{AGW} , the expression does not match observations, unless the relaxation time τ is *increased*, or the heat content N_{CL} decreased. These are contradictory adjustments: increasing τ implies a thicker, whereas lowering N_{CL} requires a thinner *climate layer*. As $\lambda_{AGW} = C_{CL}/\tau$ is fixed and C_{CL} scales with the layer thickness only, these opposing requirements create an internal inconsistency that cannot be resolved.
- dF_{TOT}/dt represents the trend in the sum of all *forcings*, calculated via dF_{TOT}/dt = λdT_S/dt + dN/dt. Since both dN/dt and dT_S/dt are derived from observations, differences in the calculated dF_{TOT}/dt are primarily due to the choice of λ. As expected, the *NAT-set* yields a slightly higher value than the *IPCC-set*. However, this difference is modest, especially considering the 3x difference in climate sensitivity between the two sets.
- N_0 is the level of the virtual radiation balance as determined from the OHC-data and can also be calculated from the warming of the *climate layer* $C_{CL}dT_S/dt = N_{CL}$. The *IPCC-set* once again fails to match this value with its unrealistically thin climate layer due to the chosen λ_{AGW} . By contrast, the *NAT-set* aligns well with the OHC observations, consistent with the earlier finding above that the $\lambda dT_S/dt$ term is physically plausible.
- dF_{NA}/dt represents the portion of total forcing not attributable to GHGs. Under the AGW-hypothesis, which recognizes only anthropogenic GHGs as forcing agents, the *IPCC-set* necessarily implies: dF_{NA}/dt = dN₀/dt. This equality indeed holds in Table 1. However, this apparent agreement is misleading. In the AGW framework dN₀/dt = 0 by definition, because natural influences are excluded. By adjusting dF_{GHG}/dt and λ_{AGW}, the energy balance equation dF_{GHG}/dt = λdT/dt + dN/dt according to the AGW-hypothesis, can always be satisfied. Section 5 already showed that such adjustments cannot overcome the fundamental requirement dN/dt < dF_{GHG}/dt, which remains a major unresolved issue in the IPCC's AGW-framework.
- dN_0/dt equals dN/dt in a true *steady state*. However, given the possibility of slowly varying natural forcings and a non-constant dT_S/dt , the OHC data since 2004 suggest a constrained relationship: $dN_0/dt \approx 0.80*dN/dt$. In the *NAT-set*, this requires a small negative adjustment to the temperature trend of about -0.003 K/year. Because dF_{TOT}/dt is fixed, that small negative contribution in (6) due to $dN_0/dt < dN/dt$, is offset by a corresponding increase in dF_{SW}/dt in the next column. Such a minor correction will not lead to essentially different conclusions.
- **dF**_{SW}/**dt** is just the "residue" of dF_{NA}/dt after subtracting dF_{GHG}/dt and dN₀/dt. In the AGW-hypothesis of the IPCC, this is zero *by definition*, since natural or non-GHG forcings are excluded. In fact, using (11), this assumption even yields a slight *cooling* effect, despite the observed increase in incoming SW-radiation. This strongly undermines the *IPCC-set*'s credibility. The *NAT-set*, on the other hand, yields dF_{SW}/dt ≈ 0.041 W/m²/year, which aligns with the observed albedo changes (see Section 8) and contributes meaningfully to *global warming*.

- **dN/dt** serves as a consistency check, computed from the sum of previous components via (7). As expected, all values check out.
- ΔT_{GHG}/ΔT expresses the GHG-share in the observed *global warming* trend, calculated as (dF_{GHG}/dt)/(λdT_S/dt). It involves only the three parameters that most clearly distinguish the *NAT-set* from the *IPCC-set*: λ, dT_S/dt and dF_{GHG}/dt. For the *NAT-set*, this ratio yields roughly 1/3rd anthropogenic and consequently, 2/3rd "natural" warming; consistent with the outcome of [4]. Even when using λ_{PL} in combination with IPCC's high values for dF_{GHG}/dt and dT_S/dt, the result still attributes over 50% to warming from natural origin. Thus, the critical discriminant is the climate sensitivity 1/λ and not so much F_{2xCO2}, the greenhouse gas strength. In contrast, the *IPCC-set* implies that 144% of the observed warming is of anthropogenic origin. Clearly, an impossible result unless a substantial, unrecognized *cooling* trend exists to offset this "overheating". Not a very plausible concept with an increasing solar radiation as observed. This again highlights how tuning of parameters like λ_{AGW} and RF_{2xCO2}, to match a specific relationship can lead to implausible outcomes elsewhere in the system.

7. The consequences of the AGW-hypothesis under a "GHG-only" scenario

The preceding analysis highlights how the IPCC's assumptions diverge significantly from observed reality. While the IPCC model components may collectively reproduce the observed warming trend, they fail to individually align with key observational data, in particular the *Ocean Heat Content*.

A useful measure here, is the ratio $\Delta T_{GHG}/\Delta T$ which quantifies how much of the observed temperature change is attributable to greenhouse gases. In the context of (11), representing the "GHG-only" scenario central to the AGW hypothesis, this ratio should approach 1 if the IPCC narrative is correct. Demonstrating this equivalence is essential to validating IPCC's framework.

7.1. Varying the temperature trend dT_S/dt

We begin by examining the surface temperature trend dT_s/dt, which in the IPCC framework is set at 0.0234 K/year, consistent with NASA's CERES-EBAF v4.2 dataset. Its previous version, v4.1, used a lower trend of approximately 0.0186 K/year. In v4.2, updated in January 2024, the trend was suddenly aligned (for unclear reasons) with the HadCRUTv5 dataset (see Section 4.3).

While this higher trend is broadly consistent with UAH-TLT data over land [18], the global average from the same satellite series yields a lower 0.015 K/year, closely matching the sea surface temperature trend from ARGO floats (Fig. 1). If we were to adopt this lower value in the *IPCC-set*, the ratio $\Delta T_{GHG}/\Delta T$ would increase to approximately 2.2, since dT_s/dt appears in the denominator. This might explain the IPCC's apparent preference for datasets with high warming trends. However, even with speculating about "accelerating" global warming, achieving $\Delta T_{GHG}/\Delta T=1$ would require a trend of 0.034 K/year, well above what is currently observed or justifiable.

7.2. Adjusting climate sensitivity $1/\lambda$

An alternative route is to increase climate sensitivity in the IPCC-set. This actually worsens the mismatch. To bring $\Delta T_{GHG}/\Delta T$ down to 1, we would need to decrease the climate sensitivity. This would imply a feedback parameter $\lambda \approx 1.6 \text{ W/m}^2/\text{K}$, corresponding to a climate sensitivity roughly twice the inverse of the *Planck feedback parameter* rather than three times larger. However, this value is not supported by *General Circulation Models* (GCMs), on which the IPCC-set is founded. In fact, the latest CMIP6 models tend toward even higher climate sensitivities than previous generations.

7.3. Modifying the GHG-forcing strength F_{2xCO2}

The third option is to adjust the *forcing* strength F_{2xCO2} . IPCC-AR6 sets this value at 3.9 W/m² [8]. To satisfy $\Delta T_{GHG}/\Delta T = 1$, it should be lowered to about 2.7 W/m². Ignoring definitional nuances (see the discussion in Section 4.4), this required value is even lower than what is derived from *clear-sky* radiative transfer calculations [22].

7.4. Altering the climate relaxation time τ

Finally, we could consider modifying the relaxation time $\tau = 4$ years, which influences several derived parameters (see Table 1). But this parameter **does not** affect the $\Delta T_{GHG}/\Delta T$ ratio. As such, it offers no pathway for reconciling the "GHG-only" scenario with the observed data.

8. The forcing trend dFsw/dt related to changes in incoming solar radiation SWIN

8.1. Changes in cloudiness

Section 6 showed that the *NAT-set* yields a residual forcing trend of approximately $dF_{SW}/dt \approx 0.041 \text{ W/m}^2/\text{year}$. Regardless of the value of F_{2xCO2} , a constant GHG forcing trend (dF_{GHG}/dt) in the LW- channel should result in a constant LW_{OUT}, as established in Section 5. Observations (Fig. 3) on the contrary, reveal not only a significant positive trend in dLW_{OUT}/dt , but an even larger one in dSW_{IN}/dt .

The solar constant (S_0) remains nearly constant on an annual basis, as confirmed by CERES data over the past 23 years. Seasonal variations, however, are non-negligible. For instance, over 18 years, the average S_0 during spring (MAM) increased by about 0.2 W/m² compared to autumn (SON). During spring in the Northern Hemisphere, high-latitude regions received ~0.4 W/m² more solar radiation than their Southern Hemisphere counterparts. These variations likely result from orbital changes and, although often dismissed, they represent potential forcings of a similar magnitude as those of GHGs. In particular, they will influence the redistribution of heat as they affect the Northern- to Southern Hemisphere balance. Nevertheless, the observed increase in SW_{IN} is primarily due to albedo changes, especially from clouds. Variations in S_0 are effectively embedded within the broader dSW_{IN}/dt trend, but they do not explain its magnitude on their own.

8.2. The Cloud Radiative Effect (CRE)

Clouds influence both SW and LW radiation fluxes in the same direction, but to different extents. This impact is known as the *Cloud Radiative Effect* (CRE). CERES data provides global average values: SW-CRE \approx 45.2 W/m², and LW-CRE \approx 25.6 W/m² respectively. These are derived from 20-years of radiation measurements under *clear-sky* (cs) and *all-sky* (as) conditions with 67% average cloud cover.

To estimate the net cloud-induced forcing from the SW_{IN} trend, we multiply dSW_{IN}/dt by the net-CRE factor, calculated as: $(1-LW-CRE/SW-CRE) \approx 0.43$ [9]. Changes in clouds and cloudiness are more than just cloud area-related effects as in this CRE. Changes in transparency, mostly for the SW-channel and changes in *Top of Cloud* (TOC) temperature for the LW-channel, contribute as well. While CERES offers some data on cloud area and TOC temperature, no robust method currently exists for incorporating these into an improved cloud forcing estimate. As such, dSW_{IN}/dt remains our best proxy for quantifying the radiative effect of cloud changes.

Clouds also affect dLW_{OUT}/dt through their shielding effect, influencing both CO₂ and water vapor forcing. The water vapor content in "*clear-sky*" conditions within an *all-sky* atmosphere, differs from that of a hypothetical Earth in a *clear-sky* equilibrium. Since a truly *clear-sky* Earth doesn't exist, interpreting the difference between *clear-sky* and *all-sky* LW_{OUT} is inherently complex [25].

Science of Climate Change

8.3. All-sky versus Clear-sky SW_{IN} data

SW_{IN} is affected by more than clouds alone. Figure 3 shows only *all-sky* (*as*) data, but the *clear-sky* SW_{IN}(*cs*) has also increased over the same period by about 0.036 W/m²/year (see Fig. 2 in [4]). This trend likely follows changes in surface reflectivity, including snow/ice melt (*Surface Albedo* feedback), changes in land-use (urbanization), and *Global Greening* (by increased CO_{2-levels?). To isolate the cloud-related effect, we subtract the *clear-sky* (*cs*) trend from the *all-sky* (*as*) value dSW_{IN}(*as*)/dt \approx 0.077 W/m²/year. Since 67% of Earth's surface is cloud-covered, only 1/3rd of this *clear-sky* trend affects the *all-sky* value, leaving a cloud-related SW_{IN} trend \sim 0.065 W/m²/year. Multiplying this by the net-CRE factor gives a cloud-related SW forcing trend dF_{SW}/dt of about 0.43*0.065 \approx 0.028 W/m²/year.}

This net-CRE ratio applied here, as well as dSW_{IN}/dt are global averages. But regional discrepancies with $SW_{IN} >> LW_{OUT}$ around the Tropics and $SW_{IN} << LW_{OUT}$ in the Polar regions, do matter. Hence, both net-CRE and dSW_{IN}/dt (as - cs) vary with latitude (see Fig. 6). The values in Fig. 6 are shown per unit area and must be cosine-weighted by latitude to yield a global average. The data suggests that the applied factor (0.43) may slightly underestimate the cloud forcing, so the derived 0.028 W/m²/year is likely conservative.

Finally, we have to add the *Surface Albedo* part of 0.012 W/m²/year again that we first subtracted to calculate the net forcing from dSW_{IN}(as)/dt, making $dF_{SW}/dt \approx 0.040 \text{ W/m}^2/\text{year}$.

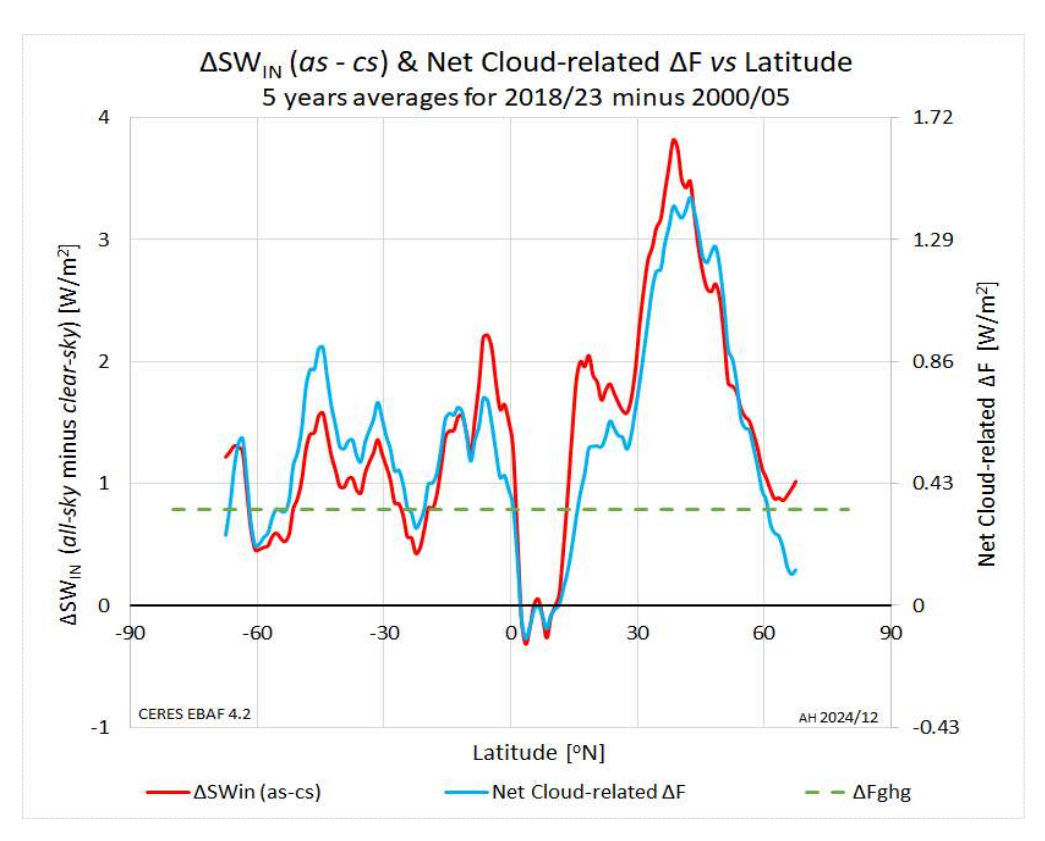


Fig. 6 Eighteen-year difference between 5-years averages of the latitude-dependent "all sky minus clear sky" incoming Solar radiation ΔSW_{IN} (as - cs) and the corresponding net cloud-related forcing ΔF_{SW} as calculated with the latitude dependent net-CRE ratio as described in Section 8. The respective vertical axes are scaled to match globally averaged net-CRE, demonstrating that this approach provides a good estimate of the global mean cloud-related forcing ΔF_{SW} . The figure highlights that this forcing is predominantly a Northern Hemisphere phenomenon, with a peak in ΔF_{SW} of approximately 1.5 W/m². For comparison: the change in GHG forcing ΔF_{GHG} over the same period was as indicated, about 0.34W/m² (or 0.70 W/m² using IPCC's RF_{2xCO2} forcing value). Data source: https://ceres.larc.nasa.gov/data [9].

8.4. Comparing dF_{SW}/dt as derived from SW_{IN} versus the calculated value from Tabel 1

The empirically derived $dF_{SW}/dt \approx 0.040~W/m^2/year$ aligns closely with the 0.041 $W/m^2/year$ obtained through the calculations used to construct Table 1. Considering the various assumptions and uncertainties involved in this derivation, this agreement is noteworthy and unlikely to be coincidental. Combining this with $dF_{GHG}/dt = 0.019~W/m^2/year$ and $\lambda = 3.3~W/m^2/K$, we calculate with (13) a temperature trend $dT_S/dt \approx 0.015~K/year$. This is consistent with both the UAH-TLT satellite data and the SST trend, affirming the *NAT-set* as a reasonable model framework.

Figure 6 also illustrates that changes in cloudiness are more pronounced on the Northern Hemisphere, especially at mid-latitudes and over Western Europe. For example, the Dutch KNMI weather-station at Cabauw (51.87°N, 4.93°E), where all ground-level radiation components are monitored every 10 minutes, recorded an increase in solar radiation of almost +0.5 W/m²/year since 2000 [26]. Applying the 0.43 net-CRE factor (conservative for this latitude), we estimate a local forcing trend dF_{SW}/dt \approx 0.2 W/m²/year. This is an order of magnitude larger than the GHG-forcing (0.019–0.037 W/m²/year). Even with the IPCC values, GHGs can just account for about 16% of the warming at this station. The average temperature trend for this rural station located in a polder largely covered by grassland, is with \sim +0.043 K/year almost 3x the global average. This, nor the other trends mentioned above can be adequately explained by the IPCC's GHG-only model. As Section 9 will show, it also fails to explain the observed trend in SW_{IN} at TOA.

9. Cloud-feedback as a possible origin of the forcing trend dFsw/dt

The IPCC places strong emphasis on the role of *climate feedbacks* in amplifying the warming effect of greenhouse gases (GHGs) [8]. These feedbacks are considered secondary consequences of *Anthropogenic Global Warming*, driven by the initial temperature increase from GHGs. Among them, *Water-Vapor* feedback is the most significant. A warmer atmosphere holds more water vapor (approximately +7%/K) and since water vapor is a potent GHG, even a small warming from CO₂ can amplify itself through enhanced evaporation.

Other feedbacks recognized by the IPCC include *Lapse Rate*, *Surface Albedo*, and *Cloud* feedbacks [8], all of which are inherently tied to the presence and behavior of water in its various phases. Therefore, these feedbacks are natural responses to temperature changes, regardless of the original cause of warming, be it GHGs, incoming solar variability, or internal effects. They are not *additive* components to natural climate sensitivity, as treated by the IPCC, but rather integral parts of it [4].

In the energy balance framework discussed in Fig. 2, feedbacks manifest through a temperature sensitive R, thus influencing how quickly the system can return to equilibrium after a perturbation. Hence, their influence on temperature. However, through $\lambda = C_{CL}/\tau$, they are already incorporated in all applied equations in this paper through the value of τ .

This conceptual distinction underlies the key difference in climate sensitivity assumptions between the *NAT-set* (natural feedback dominated, (near) Planck response) and the AGW/IPCC-set (strong positive feedbacks), as elaborated in [4].

9.1. Estimating the GHG-induced feedback contributions

In Section 8, we included the *Surface Albedo* feedback, changes in reflected solar radiation from the surface due to, for example, snowmelt or changes in vegetation. We didn't distinguish whether these were caused by warming or other factors (e.g., *land use change* or *global greening*). In the IPCC framework, however, all feedbacks, including *Albedo* and *Cloud* feedbacks, are primarily presumed to be secondary effects of GHG-driven warming. This interpretation leads to the claim that the observed increase in incoming solar radiation (SW_{IN}) is not natural but is in itself a feedback effect from GHGs, caused by temperature-induced reductions in snow- and cloud cover.

To test this idea, we can estimate the contribution of temperature-driven feedbacks, specifically from *Surface Albedo* and *Cloud* changes, to the observed trend in dF_{SW}/dt as calculated from dSW_{IN}/dt .

9.1.1. Surface Albedo feedback

From Table 1, the GHG-induced component of warming accounts for about $1/3^{rd}$ of the total. Applying this to the *Albedo* feedback trend included in dSW_{IN}/dt ($\sim 0.012~W/m^2/year$ as shown in Section 8), the GHG-induced portion is only $\sim 0.004~W/m^2/year$. With a temperature trend of 0.015 K/year, it implies a *Surface Albedo* feedback parameter $\lambda_{SA} \approx 0.3~W/m^2/K$, slightly lower than the IPCC's AR6 estimate. But even using their value $\lambda_{SA} = 0.35 \pm 0.25~W/m^2/K$, gives a maximum contribution of only 0.005 W/m²/year to dF_{SW}/dt . That is still far too small to account for the observed trend.

9.1.2. Cloud feedback

For estimating the GHG-induced *Cloud* feedback, we have no other option than to use the IPCC's AR6 estimate for $\lambda_{CF} = 0.4 \pm 0.5$ W/m²/K as derived from GCMs [8]. The sum of all temperature driven *feedbacks* is about 2.2 W/m²/K of which 2/3rd has to be attributed to *Water-Vapor* feedback [4,8]. So, the high side of the range is very unlikely. On the low side of the range, negative values for λ_{CF} will not help SW_{IN} to increase, so we limit ourselves here to the center value. With the observed surface temperature trend $dT_S/dt = 0.015$ K/year, in line with SST trends over the predominantly oceanic cloud-forming regions, we calculate a *Cloud* feedback contribution of only 0.006 W/m²/year. With only one-third of the warming attributed to GHGs, the anthropogenic share of this feedback is roughly 0.002 W/m²/year.

9.2. Combined feedback impact and implications

Combining these estimates for the GHG-induced *Surface Albedo* and *Cloud* feedbacks yield a contribution of only $\sim 15\%$ of the total dF_{SW}/dt ≈ 0.040 W/m²/year as derived in Section 8.

Specifically, Cloud feedback alone accounts for just 5% of the total, meaning it is insufficient to explain the observed increase in SW_{IN}. Furthermore, it is notable that the Cloud feedback contribution is not even larger than that from the Surface Albedo, despite clouds playing a dominant role in radiative forcing and deliver about 50% of the normal Greenhouse Effect [25]. This might be due to the fact that not all Surface Albedo changes are temperature-driven. Change of land-use and Global Greening can occur independently of GHG-induced warming, yet still influence climate/temperatures.

In conclusion, the GHG-related *Surface Albedo* and *Cloud* feedbacks are far too weak to explain the observed trend in SW_{IN} . The majority of the trend must therefore be attributed to natural causes unrelated to GHG-induced warming. The resulting forcing trend $dF_{SW/}dt \approx 0.040 \text{ W/m}^2/\text{year}$ as calculated in Section 8 using the observed $dSW_{IN/}dt$, matches well with the independently derived value of $0.041 \text{ W/m}^2/\text{year}$ from Section 7 and Table 1.

To estimate the purely natural contribution to global warming, we subtract the GHG-attributed share (about 0.006 W/m²/year) from the total dF_{SW}/dt, leaving a "net" natural forcing trend in the SW-channel of ≈ 0.035 W/m²/year. Given the GHG forcing trend dF_{GHG}/dt ≈ 0.019 W/m²/year, this leads to the conclusion that approximately $2/3^{rd}$ of the observed global warming is of natural origin, and $1/3^{rd}$ is due to anthropogenic cause such as the increase of e.g. CO_2 .

An alternative CERES-based analysis in [4] produced similarly, a 50/50 split, albeit assuming higher GHG-forcing trends. Even when using the IPCC GHG forcing values within the *NAT-set* (the "white row" in Table 1), natural contributions still dominate.

These findings indicate that the relative role of GHGs in observed warming depends more on the

assumed climate sensitivity than on the absolute magnitude of GHG forcing. Of course, that is partly due to the observations that GHGs are not at all playing the dominant role in global warming, which IPCC attributes to them. As emphasized in [4], it is then the value of climate sensitivity and not necessarily the forcing strength that most strongly determines warming outcomes.

This analysis reinforces a fundamental point: climate feedbacks are not external modifiers of climate sensitivity; rather, they are inherent to the system. Their combined effect is already embedded in the climate response function. The IPCC's treatment of feedbacks as additive components used to "explain" high sensitivities in GCMs is conceptually flawed. Physically, Earth's climate is governed by the mass balance of water in all its phases: ice, snow, liquid, vapor, and clouds. The dynamics between these phases are temperature-sensitive, and they constitute the feedback processes. Feedbacks aren't just *add-ons* to the climate system, they *are* our climate.

10. Ocean Heat Content increase

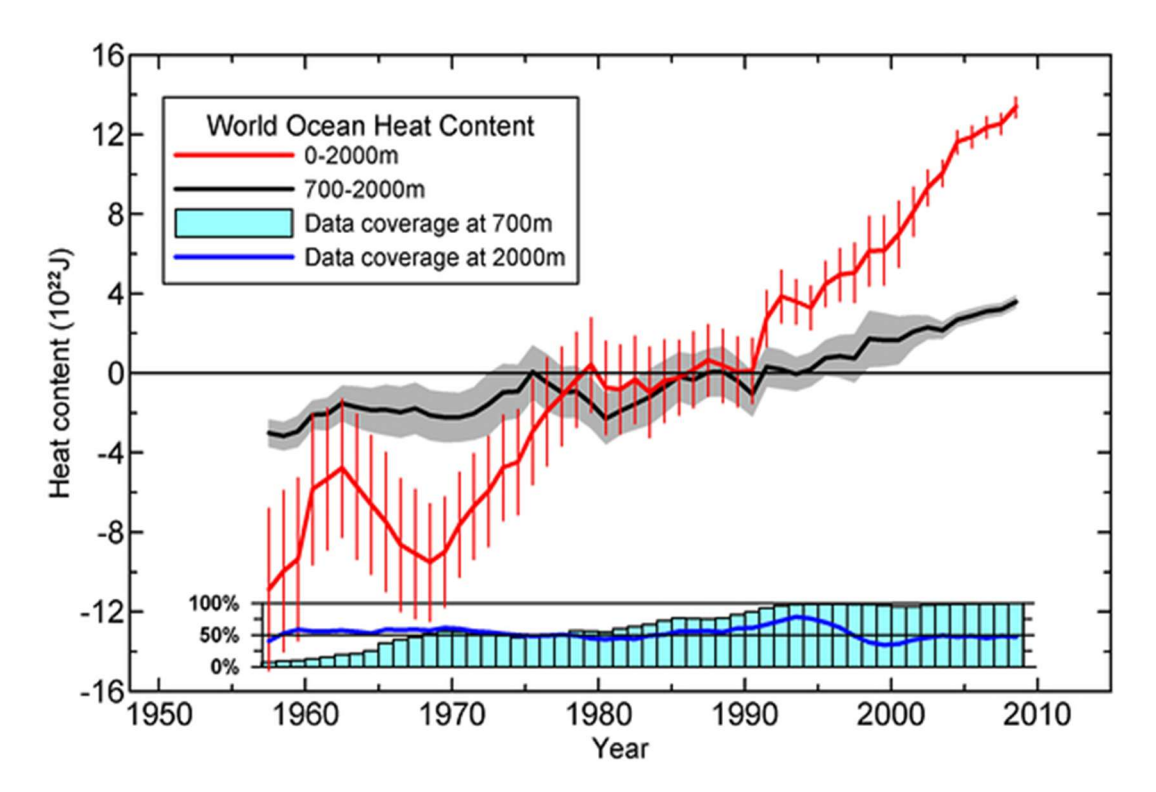
In the introduction, the "heat in the pipeline" concept: the idea that heat stored in the deep, cold ocean layers could later resurface to significantly influence surface temperatures, was challenged. Without a substantial decrease in surface temperatures to reverse ocean stratification, this seems highly unlikely. Large and rapid temperature fluctuations during the pre-industrial era with rates up to plus, but also minus 0.05 K/year over several decennia as recorded in the Central England Temperature (CET) series [27], more than three times the rate observed today, further undermine the notion of a slow-release heat mechanism dominating surface temperature trends.

Ocean Heat Content must be related to solar energy. It is the prime source of energy heating the Earth thermal system. Almost 1 W/m² of that 240 W/m² solar flux that is in average entering the system, is presently remaining in the oceans. This is an order of magnitude larger than the estimated 0.1 W/m² of geothermal heat upwelling from the Earth inner core [11]. Extra greenhouse gasses don't add energy to the system, but just obstruct cooling. As shown in Section 5.3, this accounts for a radiation imbalance offset τ dF_{GHG}/dt, or equivalent to a contribution to dOHC/dt of only about 0.08 W/m².

As redistribution of "heat in the pipeline" will not change the total OHC, roughly ¾ of the observed positive trend in OHC must at least be attributed to rising solar input. The oceans act in this way as our climate system's thermal buffer. It will mitigate warming during periods of increased solar input and dampen cooling when solar input declines, underscoring its critical role in Earth's climate stability.

Levitus *et al.* (2012) [28] combined OHC estimates back to 1955 to the data of the ARGO program as shown in Fig.7. Despite the high uncertainties in pre-ARGO ocean temperature measurements, it looks as if we had periods with a very strong positive +0.8 W/m² (1970-1980) as well as a very strong negative -0.7 W/m² radiation imbalance (1963-1970). But also, a period with an almost perfect radiation balance (1980-1990). Nevertheless, when averaged over the entire period from 1955 to 2010, the OHC trend to 2000 m depth corresponds to a positive net radiation imbalance of approximately +0.4 W/m². We also must have had a relatively high positive radiation imbalance before the turning point at $t = \zeta$, going from global cooling into a global warming regime. It all indicates to a positive radiation imbalance for most of the time, even before GHGs allegedly started to change our climate.

Reconstructed data in the AGGI database [21], show that GHG concentrations were already rising exponentially after WWII, implying a steady dF_{GHG}/dt since at least 1955. Therefore, the almost constant forcing rate from GHGs cannot have triggered these abrupt radiation imbalance shifts as visible in Fig.7. So, the sudden variations around the early 1960s, 1970, 1980 and 1990, must have been triggered by natural events. Such rapid changes in OHC, as for instance around 1970, where N changes from a negative into a positive balance by $+1.5~\text{W/m}^2$ in about 4 years of time, also indicates a rather short climate relaxation time τ . Again, this contradicts IPCC's high climate sensitivity value.



"Time series for the World Ocean of ocean heat content (10^{22} J) for the 0–2000 m (red) and 700–2000 m (black) layers based on running pentadal (five-year) analyses. Reference period is 1955–2006. Each pentadal estimate is plotted at the midpoint of the 5-year period. The vertical bars represent +/-2.*S.E. about the pentadal estimate for the 0–2000 m estimates and the grey-shaded area represent +/-2.*S.E."

Fig. 7. Graph and part of its caption reproduced from Levitus et al. [28], showing estimates of Ocean Heat Content (OHC) since 1955, including the associated 2 σ uncertainty range. At NOAA's Climate.gov, the 0–700 m OHC data are cited as evidence of greenhouse gas (GHG) effects, using the statement: "More than 90 percent of the excess heat trapped in the Earth system due to human-caused global warming, has been absorbed by the oceans".

The strong downwards slope in the OHC before 1970 confirms the observation in Section 5.4 and expressed by (12) that around the turning point $t = \zeta$, the forcing trend in the SW-channel had to be negative. Moreover, the rather slowly increasing 700-2000m OHC data in Fig.7 indicate that most of the fluctuations have occurred relatively close to the surface. Heat from *e.g. seafloor volcanism* as "warming from below", is expected to show up more pronounced in this 700-2000m OHC-profile. Although we cannot rule out *geothermal* influences [29], this observation makes them less likely.

As the OHC seems to be primarily coupled to SW_{IN}, the most plausible cause would involve rapid changes in SW-forcing. A sudden drop in cloud-cover might explain such changes, but no convincing observations could be found for the 1960-1980 period. Alternatively, changes in the latitudinal distribution of cloud-cover as illustrated by Fig.6, can result in similar radiative impacts due to the stark contrast between a positive radiation imbalance in the Tropics and a very negative imbalance at the Poles. The ENSO-oscillations in the Pacific Ocean around the equator are a typical example for such influences, as also illustrated in Fig.3 [10]. Shifts in cloud distribution are linked to changes in wind patterns and/or ocean currents, reinforcing the idea as indicated in Section 1, that even minor disruptions in horizontal heat transport can trigger major shifts in our climate's equilibrium [29, 30]. Sharp shifts in Earth's radiation imbalance like the one around 1970 as inferred from Fig.7, may even represent one of those alleged *tipping points*. But in this case, certainly not one triggered by GHGs. Ironically, some climate scientists in the early 1970s predicted an impending (Little) Ice Age [31].

While additional data (e.g. radiation measurements) are needed to draw firm conclusions, the available evidence already challenges the prevailing GHG-centric narrative again. GHG

Science of Climate Change

emissions, with their near constant forcing rate, cannot account for the timing nor the magnitude of historical OHC trends, as NOAA explicitly suggests [32]. Similarly, claims by KNMI that "accelerations" in radiation imbalance trends are GHG-driven [1], are not supported by data. And finally, the alarms around "heat in the pipeline" must be exaggerated if not totally misplaced. Given the similarities in radiation imbalance and GHG forcing rates around 1970 with today's situation, we must conclude that this assumed heat manifested itself at that time apparently as "cooling in the pipeline".

However, warnings for continued warming even if we immediately stop now with emitting GHGs are nevertheless, absolutely justified. Only, it isn't warming then from that *heat in the pipeline* due historical emissions that will boost our temperatures. Warming will continue to go on as long as *natural forcings* will be acting. These are already today's dominant drivers behind global temperature trends. And unfortunately, they will not be affected by the illusion of stopping global warming as created by implementing *Net-Zero* policies.

11. Summary and conclusions

This analysis demonstrates that a *global warming* scenario driven solely by *greenhouse gases* (GHGs) is inconsistent with more than 20 years of observations from space and of *Ocean Heat Content*. The standard *anthropogenic global warming* (AGW) hypothesis, which attributes all observed warming to rising GHG concentrations, particularly CO₂, cannot explain the observed trends. Instead, natural factors, especially long-term increase in incoming solar radiation, appear to play a significant and likely dominant role in global warming since the mid-1970s.

The observed increase in incoming solar radiation cannot be accounted for by the possible anthropogenic side effects of *Albedo*- and *Cloud*-feedback. All evidence points to the conclusion that this "natural" *forcing* with a trend of about 0.035 W/m²/year is equal to, or even exceeds the greenhouse gas related *forcing* of about 0.019 W/m²/year. Based on these values, only 1/3rd of the observed temperature trend can be of anthropogenic origin. The remaining 2/3rd must stem from *natural* changes in our climate system, or more broadly, in our entire Earth' thermal system.

Moreover, the observed increase in Earth's radiation imbalance appears to be largely unrelated to GHGs. Instead, it correlates strongly with natural processes driving increased incoming solar radiation. Claims of "acceleration" in the radiation imbalance due to GHG emissions are not supported by the trend in accurately measured GHG concentrations. If any acceleration in global warming is occurring, it is almost certainly driven by the increasing flux of solar energy—an inherently natural phenomenon not induced by greenhouse gases.

In summary, this analysis challenges the notion that GHGs are the primary drivers of recent climate change. It underscores the importance of accounting for natural variability, especially in solar input, when interpreting warming trends and evaluating climate models.

Funding: No funding received, nor solicited.

Co-Editor: Stein Storlie Bergsmark; Reviewers: Anonymous

References

- 1. https://www.knmi.nl/over-het-knmi/nieuws/wat-iedereen-zou-moeten-weten-over-de-op-warming-van-de-aarde (in Dutch)
- 2. Hansen, J. *et al.* (2023), *Global Warming in the Pipeline*, Oxford Open Climate Change, **3(1)**, https://doi.org/10.1093/oxfclm/kgad008)

- 3. Trenberth K.E. and Caron J.M. (2001), Estimates of Meridional Atmosphere and Ocean Heat Transports, J. Climate 14, 3433–3443, https://doi.org/10.1175/1520-0442(2001)014%3C3433:EOMAAO%3E2.0.CO;2
- 4. Huijser, A. (2024), *Greenhouse Feedbacks are Intrinsic Properties of the Planck Feedback Parameter*, Science of Climate Change **4.2**, 89-113, https://doi.org/10.53234/scc202411/03
- 5. Schwartz, S. E. (2007), *Heat capacity, time constant, and sensitivity of Earth's climate system,* J. Geophys. Res., 112, https://doi.org/10.1029/2007JD008746
- 6. https://argo.ucsd.edu/
- 7. https://www.ncei.noaa.gov/access/global-ocean-heat-content/basin heat data.html
- 8. Climate Change (2021), *The Physical Science basis IPCC WG 1*, 6th Assessment Report, Technical Summary TS3.2 pg.93-97, http://www.ipcc.ch/report/ar6/wg1
- 9. https://ceres.larc.nasa.gov/data
- 10. ENSO MEIv2: https://psl.noaa.gov/enso/mei/
- 11. Pollack H.N., Hurter S.J. and Johnson J.R. (1993), Heat flow from the Earth's interior: Analysis of the global data set, Rev. Geophys. 31, 267-280, https://doi.org/10.1029/93RG01249
- 12. https://www.britannica.com/science/marine-ecosystem#ref588433
- 13. Treguier A.M. et al (2023), The mixed-layer depth in the Ocean Model Intercomparison Project (OMIP), Geosci. Model Dev. 16, 3849, https://doi.org/10.5194/gmd-16-3849-2023
- 14. https://www.climate4you.com/: the oceans paragraph
- Lewis, N. & Curry, J. (2015), The implications for climate sensitivity of AR5 forcing and heat uptake estimates. Clim Dyn 45, 1009–1023 https://doi.org/10.1007/s00382-014-2342-v
- 16. For a good overview of the various temperature trends, their quality, pros/cons, etc., see https://www.climate4you.com/"global temperatures"
- 17. https://www.metoffice.gov.uk/hadobs/hadcrut5/data/HadCRUT.5.0.2.0/download.html
- 18. https://www.nsstc.uah.edu/climate/index.html
- 19. Spencer R., Christy J. & Braswell W. (2025), *Urban Heat Island Effects in U.S. Summer Surface Temperature Data*, 1895-2023, accepted by JAMC in April 2025. https://doi.org/10.1175/JAMC-D-23-0199.1
- 20. https://www.metoffice.gov.uk/hadobs/hadsst4/
- 21. https://data.giss.nasa.gov/modelforce/ in more detail: https://gml.noaa.gov/aggi/aggi.html
- 22. Van Wijngaarden W. & Happer W. (2021), *Relative Potency of Greenhouse Molecules*, https://doi.org/10.48550/arXiv.2103.16465
- 23. Rentsch C. (2021), Radiative forcing by CO₂ observed at top of atmosphere from 2002 to 2019 (v2), https://doi.org/10.48550/arXiv.1911.10605 or https://essopenarchive.org/users/283962/articles/607772-radiative-forcing-by-co-observed-at-top-of-atmosphere-from-2002-2019
- 24. MODTRAN, https://climatemodels.uchicago.edu/modtran/
- 25. Huijser A., unpublished results
- 26. https://en.wikipedia.org/wiki/KNMI-mast_Cabauw
 KNMI's hourly and daily averaged data from station # 348: https://daggegevens.knmi.nl/
- 27. See the *Central England Temperature* (CET) series of temperatures measured using thermometers since 1659, with decennia-long changes up to $|dT_s/dt| \approx 0.05$ K/year. https://hadleyserver.metoffice.gov.uk/hadcet/index.html

- 28. Levitus S. et al (2012), World ocean heat content and thermosteric sea level change (0-2000 m), 1955-2010, Geophys. Res. Lett. 39, L10603 https://doi.org/10.1029/2012GL051106
- 29. Mullarney J.C., Griffiths R.W. and Hughes G.O. (2006), *The effects of geothermal heating on the ocean overturning circulation*, Geophys. Res. Lett. **33**, L02607 https://doi.org/10.1029/2005GL024956
- 30. Gray B.(2018), Flaws in applying greenhouse warming to Climate Variability, https://theg-wpf.org/publications/bill-gray-flaws-in-applying-greenhouse-warming-to-climate-variabil-ity/
- 31. https://www.newscientist.com/article/mg19225822-300-the-ice-age-that-never-was/
- 32. https://www.climate.gov/news-features/understanding-climate/climate-change-ocean-heat-content